A Density Functional Study of the Various Forms of UN_4O_{12} Containing Uranyl Nitrate

Joel J. Berard, Grigory A. Shamov, and Georg Schreckenbach*

Department of Chemistry, University of Manitoba, Winnipeg, Manitoba R3T 2N2, Canada

Received: May 14, 2007; In Final Form: July 30, 2007

In this paper we report the computational results of a density functional study of 73 UN_4O_{12} isomers containing uranyl nitrate, $UO_2(NO_3)_2$, as a component. The isomers are grouped into three categories and 19 types. Forty-four isomers of 14 types are dinitrogen tetroxide adducts of uranyl nitrate, $UO_2(NO_3)_2{\cdot}N_2O_4$, 22 are nitrosonium salt adducts of uranyl nitrate, $NO^+UO_2(NO_3)_3^-$, $NO^+UO_2(NO_3)_2O(NO_2)^-$, $NO^+UO_2(NO_3)_2(ONOO)^-$, or $(NO^+)_2UO_2(NO_3)_2O_2^{2-}$, and 7 are bis(nitrogen dioxide) adducts of uranyl nitrate, $UO_2(NO_3)_2{\cdot}2NO_2$. The 22 most stable isomers in solution, representing the 20 most stable gas-phase isomers, were selected for analysis. Of these selected structures only two categories and six types were represented. Structures, frequencies, gas-phase and solution energetics, atomic charges, dipole moments, and the bonding within the N_2O_4 unit and between NO^+ and $UO_2(NO_3)_3^-$ components have been analyzed in detail. On the basis of relative Gibbs free energy calculations five isomers (the N_2O_4 adducts **a1**, **a2**, and **a3** and the nitrosonium salts **b1** and **b2**) were identified as strong candidates to exist and possibly predominate in the gas phase, with **a1** and **a2** being the strongest candidates. Similarly, four isomers (**a6**, **a5**, **a8**, and **a1**, all of them N_2O_4 adducts) were identified as strong candidates to exist and possibly predominate in a nonaqueous solution of nitromethane/dinitrogen tetroxide. Of these, **a6** was determined to be the most likely candidate to predominate in solution. The possibility of dissociation in solution has been addressed briefly. In addition, computational evidence for the existence of four new N_2O_4 isomers **20**, **22**, **27**, and **28** in both the gas and the solution phases is presented for the first time.

I. Introduction

Often the topics of computational research papers are based on existing chemical structures discovered through experimental investigations by either trial and error methods or by the unexpected chance of recognizing something unusual and exploring it further. It seems that a reversal of this process may now be possible with computational chemistry becoming poised to supply experimental chemists with alternatives for exploring new chemistry or for predicting the existence of new structures. Actinide chemistry in particular with its relatively unexplored f-element chemistry and inherent experimental challenges currently merits further investigation, and computational chemistry now offers unique advantages that can often result in time savings for experimentalists.[1−5]

With the radioactive waste and groundwater contamination that have resulted from decades of atomic weapons production and nuclear power generation, the chemistry of the early actinides is related to one of the most pressing environmental challenges of our time. Cause for concern exists if the actinides in radioactive wastes are introduced into the environment due to their toxicity and, in particular, due to the long half-lives of some of their isotopes and those of their daughter elements.[6]

Furthering the understanding of the chemistry of the early actinide elements, specifically U, Np, Pu, and Am, is among our main research interests. These elements have been explored to a much lesser extent than those before them in the periodic table. With all of the actinides being radioactive and most of them either scarce or toxic they are often found to be difficult to study experimentally. This creates an opportunity for computational studies to supplement some of the experimental efforts or potentially allow experimentalists to be better informed and prepared to make time-saving decisions before proceeding experimentally. The early actinides are among the heaviest elements, containing 90 electrons or more. This is before considering their molecular forms, thus often leading to very time-consuming calculations. With the 6p, 5f, 6d, and 7s orbitals of these elements all being relatively close in energy and spatial extent[3,7] the possibility of entirely new bonding schemes often exists.[8] As well, to approach chemical accuracy (less than 2 kcal/mol) it is necessary to include electron correlation effects, resulting from electron−electron interactions. Even more importantly scalar and often also spin−orbit relativistic effects must be included.[1−5]

Hexavalent uranium is known to exist most often in aqueous environments as the uranyl dication[7,9,10] UO_2^{2+} and is thought to combine with nitrates, when they are made available, to form the neutral complex uranyl nitrate, $UO_2(NO_3)_2$, or one of its hydrated forms $UO_2(NO_3)_2{\cdot}6H_2O$, $UO_2(NO_3)_2{\cdot}3H_2O$, or $UO_2(NO_3)_2{\cdot}2H_2O$.[11−13] Uranyl nitrate is considered to be the most abundant salt found in the reprocessing of spent nuclear fuel.[14]

Pasilis et al.[15] recently used electrospray ionization (ESI) and Fourier transform ion-cyclotron resonance mass spectrometry (FT-ICR-MS) to analyze the ions generated from uranyl nitrate solutions. In particular, with a negative ion ESI-MS of a 95:5 CH_3OH/H_2O solution, the three most intense peaks were assigned to $[UO_2(O)(NO_3)_2]^-$, $[UO_2(O)(NO_3)]^-$, and $[UO_2(NO_3)_3]^-$, respectively. The third of these gas-phase ions is identical to that of the solution-based trinitratouranylate known to form in ketones, ethers, and alcoholic solvents and is

* Author to whom correspondence should be addressed. E-mail: schrecke@cc.umanitoba.ca.

10.1021/jp073688b CCC: $37.00
Published on Web 10/04/2007

an indication of competition between solvent and nitrate molecules for ligand coordination positions to uranyl in solution.[15,16]

In the crystal structures of $K[UO_2(NO_3)_3]$, $Rb[UO_2(NO_3)_3]$, and $Cs[UO_2(NO_3)_3]$ each nitrate is found to chelate bidentately to uranyl, forming a hexagonal bipyramid around uranium.[17] The coordination of the complex ion $[UO_2(NO_3)_3]^-$ is thought to be similar in the gas phase.[15] Other relevant structures also include the previously investigated nitrosonium nitratometalates: $NO[Cu(NO_3)_3]$,[18] $NO[Co(NO_3)_3]$,[19] $NO[Ni(NO_3)_3]$,[20] and $NO[Mn(NO_3)_3]$.[21]

Furthermore, the possibility of various ionic or radical nitrogen oxides (N_xO_y) and oxoions (N_2O, NO^-, NO, $(NO)_2$, N_2O_3, NO^+, NO_2^-, NO_2, N_2O_4, N_2O_5, NO_2^+, and NO_3^-) combining with $UO_2(NO_3)_2$ leads to a multitude of diverse structures existing in equilibrium. Due to their environmental role in the chemistry of the Earth's troposphere and stratosphere and their links to ozone depletion and smog formation, nitrogen oxides have been the subject of considerable theoretical and experimental work over the past decade. Nitrogen oxides, often cited as NO_x, are produced when fossil fuels are burned and constitute a large portion of industrial pollution. The photodissociation of N_2O_4, for example, has aroused particular interest in atmospheric chemistry.[22] As well, interactions between water and N_xO_y species in condensed phases also play an important role in atmospheric chemistry. In this instance N_2O_5 has been implicated in stratospheric ozone depletion.[23−25]

The idea of computationally investigating the structural forms of UN_4O_{12} containing uranyl nitrate was prompted by a recent paper by Crawford and Mayer.[26] The authors make reference to the importance of establishing whether the uranium(VI) species of UN_4O_{12} takes on the form of an ionic or covalent compound in solution. They go on to point out how conflicting evidence for two structural forms of UN_4O_{12} appear in the research literature. The most commonly cited form is an adduct of uranyl nitrate and dinitrogen tetroxide, $UO_2(NO_3)_2 \cdot N_2O_4$, whose thermal decomposition leads to the formation of the important precursor anhydrous uranyl nitrate. The hydrated complex, $UO_2(NO_3)_2 \cdot 6H_2O$, is one of the most important compounds of the plutonium uranium recovery by extraction (PUREX) process for the separation of fission products from uranium and plutonium fuels and a main wastewater pollutant.[7] The second most cited form is the nitrosonium salt, $NO^+UO_2(NO_3)_3^-$. They were able to experimentally prepare solid-state crystals of this salt. By deposition of uranium metal turnings in a 30:70 nitromethane/dinitrogen tetroxide (CH_3NO_2/N_2O_4) solution under anhydrous conditions a precipitate was obtained from a saturated solution at −28 °C.[27]

The present computational work was undertaken with the aim of establishing, if possible, the UN_4O_{12} structure or structures containing uranyl nitrate most likely to exist and predominate in either an inert gas or a nonaqueous solution environment. As a broader goal we look to show that a computational density functional (DFT)[28] investigation into isomers of UN_4O_{12} can provide experimentalists with a valuable list of potential structural candidates for identification. An analysis of selected structures based on relative Gibbs free energies is made to identify distinguishing features that could be potentially helpful to experimental identification. Such molecular properties as the nature of bonding, relative Gibbs free energies, dipole moments, bond lengths and angles, bond orders, atomic charges, frequencies, and metal coordination are addressed and compared to experimental results where possible.

II. Computational Methods

Only recently with advances in computing power and the growing acceptance of DFT methods, which incorporate electron correlation and relativistic effects, have computational chemical investigations into intermediate size structures (containing greater than 15 non-hydrogen atoms) involving actinide elements become commonplace.[29,30] With DFT implicitly including electron correlation effects and various methods existing for incorporating relativistic effects, in addition to the time-saving advantages, one can see why DFT has recently become the quantum mechanical method of choice for computational research into actinide complexes.[1−5,31]

Gas-phase calculations were performed with Priroda-5 (p5)[32−35] and Gaussian 03 (g03).[36] All calculations used DFT with either the pure generalized gradient approximation (GGA)[31] functional PBE[37] of Perdew, Burke, and Ernzerhof or the hybrid B3LYP exchange−correlation (XC) functional.[38−40] B3LYP combines a nonlocal Becke and exact exchange functional[38] with the Lee, Yang, and Parr correlation functional.[39] Vibrational frequencies were calculated to obtain thermochemistry data, such as Gibbs free energies and corrections, and to verify the nature of stationary points of optimized geometries. All p5 calculations used correlation-consistent polarized valence triple-ζ (cc-pVTZ) basis sets.[34] As for g03, we used the cc-pVTZ basis set for nitrogen and oxygen and the Stuttgart−Dresden SC-ECP[41] basis set for uranium.

Our experience has shown that the use of pure GGA functionals yields reasonable calculation times while providing accurate geometry optimizations and reliable self-consistent field (SCF) convergences.[42,43] Frequency calculations using p5 PBE were then performed on the gas-phase p5 PBE optimized geometries to verify that no imaginary frequencies were present. Gibbs free energy corrections were obtained with these frequency calculations. B3LYP has been shown to be more accurate than PBE for the calculation of Gibbs free energies,[43,44] but due to the costs of running B3LYP optimizations, we chose to add the p5 PBE gas-phase Gibbs free energy corrections to B3LYP single-point SCF energy results obtained for both p5 and g03 before calculating relative Gibbs free energies from them. In Gaussian, an "ultrafine" integration grid and a "tight" SCF convergence criteria were used to obtain single-point SCF energies. Although this method is less than ideal, our test calculations showed that this time-saving procedure provides a good approximation for the comparison of relative Gibbs free energies.

To approximate relativistic effects in Gaussian we chose to use "small-core" effective core potentials (SC-ECPs)[41] rather than "large-core" (LC-ECPs) ones. Recently, SC-ECPs have been shown to give a much closer agreement with experiment for a number of molecular properties, including geometries,[43,45,46] vibrational frequencies,[45,46] and NMR chemical shifts.[44,47−49] Batista et al.[44] have shown that the use of SC-ECPs, along with the hybrid B3LYP[38−40] XC functional, give excellent results for the geometries, vibrations, and first bond dissociation energies of UF_6. In Gaussian, relativistic effects were included by replacing the core electrons of uranium with a Stuttgart−Dresden SC-ECP according to Küchle et al.[41] The Stuttgart−Dresden SC-ECP treats 60 electrons as the core and the remaining electrons as part of the variational valence space. Priroda applies a relativistic scalar four-component process, where all spin−orbit terms are separated from their scalar terms[34,50] and neglected.[32−35,51] For geometries and frequencies, neglecting spin−orbit effects is generally accepted to be a valid approach. In previous studies of these relativistic methods it

was found that g03 SC-ECP (60e) and Priroda's scalar four-component method were of comparable quality.[42,43]

Modeling such chemical structures in solution requires the use of accurate solvation methods. The solid-state crystals isolated[26] were found to react with both water and air, leading to the vigorous liberation of gaseous NO_2. In fact, it was determined to be so sensitive that it was deemed necessary to handle it under an inert atmosphere. We therefore chose to perform our solvation calculations with the aprotic polar solvent nitromethane (dielectric constant $\epsilon = 38.2$). Relative Gibbs free energies using this solvent were found to be very similar to those found using water as a solvent. Accurate solvated Gibbs free energy differences were obtained with single-point calculations of p5 PBE gas-phase optimized geometries using g03 B3LYP SC-ECPs and the conductor polarized continuum model (CPCM).[52] As well, using the Gibbs free energy corrections obtained from the p5 PBE gas-phase frequency results to calculate the relative solvated Gibbs free energies provided an accurate alternative to running costly g03 solvated frequency calculations. Although common, the use of single-point calculations on gas-phase optimized geometries is not considered to be the optimal method for obtaining solution-phase Gibbs free energies. A preferable method of obtaining Gibbs free energies would be to reoptimize the gas-phase geometries in solution. Efforts were made toward this using the Amsterdam density functional (ADF)[53−55] software with the scalar relativistic ZORA[56−59] method, the TZP basis set made up of Slater-type orbitals (STOs), and the conductor-like screening model (COSMO).[60−62] For ADF/COSMO calculations we used the Klamt atomic radii of 1.72 Å for oxygen and 1.83 Å for nitrogen[61] and an atomic radius of 1.70 Å for the uranium atom.[42] Due to problems with numerical noise and despite several attempts, only three of 22 isomers were found to converge to a stationary point without any imaginary frequencies. Combinations of ADF integration values and geometry gradient convergence criteria of $4.0/1 \times 10^{-2}$, $5.5/1 \times 10^{-3}$, and $6.5/1 \times 10^{-3}$ (over 22 UN_4O_{12} isomers were calculated with this last combination) were tried and found to provide similar results for imaginary frequencies (ranging from 9i to 533i in multiples of 1−4 per isomer) with no apparent advantages. We therefore chose not to pursue geometry optimizations in solution any further.

Gas- and solution-phase calculations were also performed to obtain the relative Gibbs free energies of 13 N_2O_4 isomers to discuss their relative stabilities and geometries. Relativistic methods were not necessary and we chose to use g03 B3LYP/cc-pVTZ in the gas phase and g03 B3LYP/cc-pVTZ/CPCM in solution for geometry optimizations and frequency calculations.

All molecular species calculated with uranium considered it to be in the U^{VI} oxidation state with an f^0 valency, and therefore all calculations were done with a restricted, closed-shell, Kohn−Sham formalism. Due to the biradical nature of some of the N_2O_4 isomers and the UN_4O_{12} isomers containing them as components, the use of a restricted, closed-shell formalism may not model some of the higher-energy structures effectively.

III. Results and Disscussion

The proceeding sections are organized as follows: Subsection A outlines and discusses the characteristics of the key structural components found to make up the UN_4O_{12} isomers containing uranyl nitrate, subsection B discusses how 73 identified UN_4O_{12} isomers containing uranyl nitrate are classified into three categories and 19 types, subsection C gives a general analysis and discussion of 22 select gas- and solution-phase UN_4O_{12} isomers containing uranyl nitrate, and subsection D provides a detailed by-type discussion of these isomers for the two categories and six types that were found to be represented. Finally, in subsection E, we look briefly at the possibility of dissociation of UN_4O_{12}.

TABLE 1: Calculated Gas- and Solution-Phase Single-Point Relative Gibbs Free Energies and Absolute Gibbs Free Energy Differences between Gas- and Solution-Phase ΔG_{solv} of 30 Selected UN_4O_{12} Isomers (in kcal/mol)

	p5 PBE	p5 B3LYP	g03 B3LYP	g03 CPCM B3LYP (p5)	
isomers	G^{rel}_{gas}	G^{rel}_{gas}	G^{rel}_{gas}	G^{rel}_{soln}	ΔG_{solv}
a6	8.2	2.5	3.0	0.0	−21.2
a5	8.6	2.4	3.3	1.1	−20.3
a8	7.0	2.6	3.6	2.2	−19.5
a1	0.0	0.0	0.0	3.6	−14.5
a27	19.3	18.5	17.8	4.5	−31.5
a2	1.0	0.2	−0.2	5.2	−12.8
a13	8.7	4.5	4.4	5.6	−17.0
a10	9.9	3.0	3.3	6.0	−15.4
a14	8.5	4.5	4.6	6.3	−16.5
a7	2.2	2.5	2.7	6.8	−14.7
a9	2.6	2.9	3.0	6.8	−18.3
a4	7.9	2.1	2.5	7.4	−17.0
a16	11.9	5.5	5.6	7.6	−20.6
b6	19.2	15.7	15.5	8.2	−31.1
b2	6.5	1.7	3.8	8.2	−13.8
b1	3.9	1.4	4.2	8.8	−13.5
a3	1.5	1.2	0.9	9.0	−14.0
a12	9.5	4.1	4.8	9.1	−17.5
b3	5.3	2.6	5.5	9.6	−19.1
a11	8.7	3.7	4.4	10.0	−15.5
b4	5.9	3.6	6.1	10.4	−20.1
a15	11.6	4.8	4.7	10.4	−18.4
a17	9.5	7.0	9.6	14.9	−24.6
a18	8.5	8.6	8.7	14.9	−16.2
a20	15.5	12.5	12.4	16.9	−15.6
a19	9.4	9.3	9.9	17.8	−11.9
a21	15.6	13.0	13.1	18.2	−15.5
b5	11.7	11.1	14.3	21.0	−11.4
c1	16.9	19.1	22.2	32.0	−22.6
b7	20.4	23.7	27.5	38.6	−11.2

With some exceptions (for example, isomers **a1**−**a3**, **a7**, and **a9**) the p5 PBE gas-phase relative Gibbs free energy calculations were found to be less stable as compared to both the p5 and the g03 B3LYP single-point results (Table 1). Moreover, experience shows that hybrid functionals such as B3LYP are preferable to GGAs (such as PBE) for the energetics of actinide species.[45−47] We therefore chose to use the p5 B3LYP single-point results to determine the stability ordering of the UN_4O_{12} isomers containing uranyl nitrate in the gas phase. We could just as easily have chosen our g03 G^{rel}_{gas} results instead. The two sets of results are very similar, with a few possible exceptions such as **b1**−**b4**. The two single-point B3LYP gas-phase methods appear to calculate the ionic charge separation somewhat differently, and it is difficult to tell which method is more accurate.

Thirty of the gas-phase optimized isomers with the lowest relative Gibbs free energies within each category were then chosen to calculate single-point solvated relative Gibbs free energies. The 22 lowest relative Gibbs free energy structures found in solution were then selected for detailed analysis and discussion.

Several other gas-phase isomers of UN_4O_{12} that do not contain uranyl nitrate were also identified. The most prominent one, $U(NO_3)_4$ with the formal oxidation state for uranium of IV, is as yet undiscovered, as far as we can determine.[63] However, previous experimental attempts have shown that $U(NO_3)_4$ may

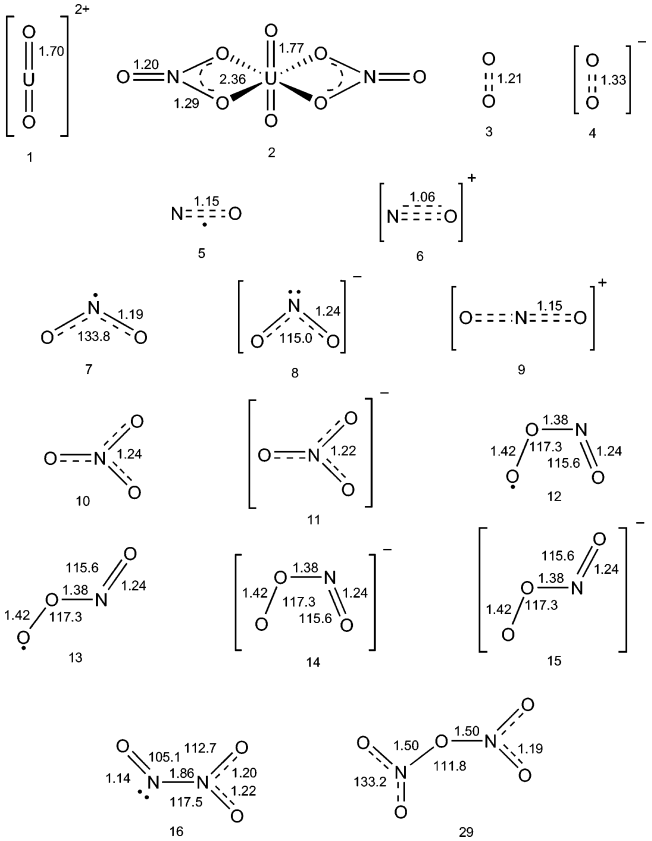

Figure 1. Structural components: **1**, uranyl dication; **2**, uranyl nitrate; **3**, dioxygen; **4**, superoxide anion; **5**, nitric oxide radical; **6**, nitrosonium (nitrosyl) cation; **7**, nitrogen dioxide radical; **8**, nitrite anion; **9**, nitronium (nitryl) cation; **10**, nitrate radical; **11**, nitrate anion; **12** and **13**, *cis*- and *trans*-peroxynitrite radical; **14** and **15** *cis*- and *trans*-peroxynitrite anion; **16**, dinitrogen trioxide; **29**, dinitrogen pentoxide. (Bond lengths are given in angstroms, and angles in degrees; see the text.)

exist in solution but was found to oxidize spontaneously to a U^{VI} complex before being isolated.[64] Our calculations show that $U(NO_3)_4$ has a gas-phase Gibbs free energy of 34.6 kcal/mol relative to our chosen reference **a1**. This high relative energy could explain the difficulty in isolating this isomer in experimental investigations. The most stable of the remaining isomers had a relative gas-phase Gibbs free energy of 62.1 kcal/mol. Consequently these isomers were not investigated any further.

A. Structural Components. A diverse assortment of nitrogen oxoions and oxides, along with dioxygen and superoxide, were found to bind with uranyl nitrate to yield the large number of computationally stable UN_4O_{12} isomers obtained. Many known nitrogen oxides, often with unusual structures, are commonly found in both ionic and radical forms. All of them contain some form of resonance hybrid/multiple bonding structure. Some of the most commonly encountered oxoions and oxides of nitrogen are NO^+, NO_2^+, NO_2^-, NO_3^-, NO, NO_2, N_2O_3, N_2O_4, and N_2O_5, with formal oxidation numbers for nitrogen ranging from +2 to +5. Other less commonly encountered forms are *cis*- and *trans*-ONOO and $ONOO^-$, the NO_3 radical, and other isomers of N_2O_3, N_2O_4, and N_2O_5 (Figures 1 and 2).[65,66] The paper by Laane and Ohlsen[67] provides a good preliminary overview of the N_xO_y species.

The majority of the bond lengths in Figure 1 are experimental, taken from one of the following references.[65,74] The exceptions are: (1) the uranyl **1** bond length, which is a calculated value using the Stuttgart SC-ECP (60e) for uranium and the DFT/B3LYP/TZVP combination for oxygen and nitrogen,[68,69] (2) the uranyl nitrate **2** bond lengths, which were calculated using the

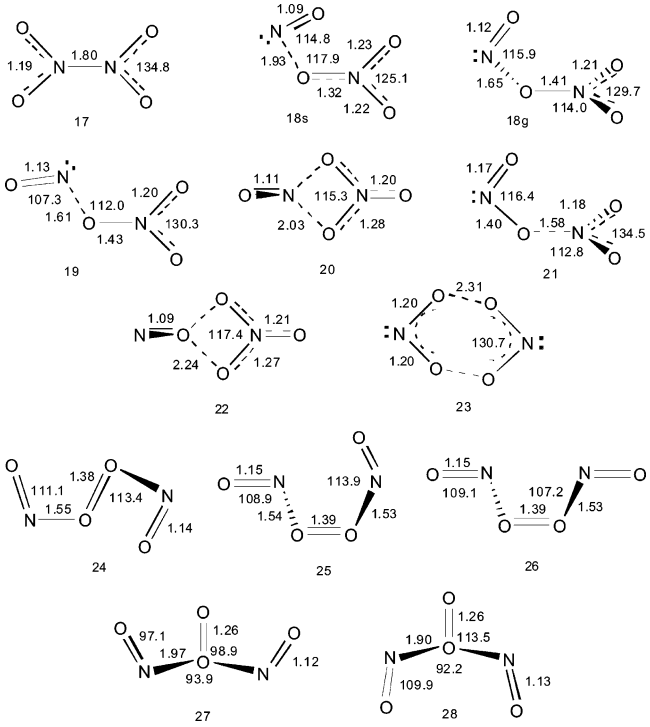

Figure 2. Thirteen isomers of dinitrogen tetroxide, N_2O_4: **17**, sym-N_2O_4; **18s**, *cis*-ON·O·NO_2; **18g**, twist-ON·O·NO_2; **19**, *trans*-ON·O·NO_2; **20**, ON·O_2NO; **21**, perp-ON·O·NO_2; **22**, $NO^+NO_3^-$; **23**, NO_2·O_2N; **24**, *cis*,*cis*-ON·OO·NO; **25**, *cis*,*trans*-ON·OO·NO; **26**, *trans*,*trans*-ON·OO·NO; **27**, *cis*,*cis*-OO·$(NO)_2$; **28**, *trans*,*trans*-OO·$(NO)_2$. (Bond lengths are given in angstroms, and angles in degrees. These are g03 B3LYP/cc-pVTZ gas-phase values; see the text.)

Stuttgart SC-ECP (60e) for uranium and the DFT/SVWN/TZVP combination for oxygen and nitrogen,[68,69] (SVWN combines a Slater exchange functional[70] with the Vosko, Wilk, and Nusair correlation functional[71]), and (3) the peroxynitrites **12**−**15**, which are CCSD(T) calculated values.[72]

In the following paragraphs a more detailed discussion of the various N_2O_4 structural forms is provided along with a brief review of some of the known chemistry of N_2O_4. The structural components of Figure 1 are discussed in the Supporting Information.

The ordering of the various N_2O_4 isomers shown in Figure 2 is based on our relative Gibbs free energy calculations with g03 B3LYP/cc-pVTZ/CPCM using a nitromethane solvent (Table 2). The nature of each stationary point was verified for 12 of 13 (**18g** was found to exist only in gas phase) structures in solution. The order of the gas-phase relative Gibbs free energies of these isomers using g03 B3LYP/cc-pVTZ was determined to be **17**, **21**, **20**, **18g**, **22**, and **24**−**28** with **19** and **23** found to be transition states with single imaginary frequencies. However, recent gas-phase calculations by Olson et al.[73] using g98 B3LYP/6-311G* (without zero-point energy corrections) and CBS-QB3 found the order to be **17**, **19**, **21**, and **23**−**26** with **18g**, **20**, **22**, **27**, and **28** unconsidered. Calculated structural parameters (g03 B3LYP/cc-pVTZ, gas phase) for all 13 structures can be found in Figure 2.

Two NO_2 radicals are thought to dimerize reversibly at low temperatures to the most common sym-N_2O_4 (O_2N·NO_2) isomer **17**, Figure 2, of D_{2h} symmetry (reaction I).[74] It is thought that the odd electron delocalizes to a π-antibonding orbital. The similarity between N_2O_4 and NO_2, with the same N═O bond length of 1.19 Å and ONO angles of 135.4° and 133.8°, respectively, along with the longer than ordinary N−N bond distance of 1.78 Å, supports the notion that sym-N_2O_4 is formed

TABLE 2: Calculated Gas- and Solution-Phase Optimized Relative Gibbs Free Energies of Free Dinitrogen Tetroxide Isomers[a]

		g03 B3LYP cc-pVTZ	g03 CPCM B3LYP cc-pVTZ	g98 B3LYP 6-311G* CBS-QB3[b]
N_2O_4 isomers		G^{rel}_{gas}	G^{rel}_{soln}	E^{rel}_{gas}
sym-N_2O_4	**17**	0.0	0.0	0.0
cis-ON·O·NO_2	**18s**		5.7	
twist-ON·O·NO_2	**18g**	11.9		
trans-ON·O·NO_2	**19**	(10.3)	7.0	3.4
ON·O_2NO	**20**	11.8	7.6	
perp-ON·O·NO_2	**21**	11.6	11.8	7.4
$NO^+NO_3^-$	**22**	33.0	18.3	
NO_2·O_2N	**23**	(22.0)	23.1	13.4
cis,*cis*-ON·OO·NO	**24**	30.8	30.3	24.0
cis,*trans*-ON·OO·NO	**25**	32.3	34.3	25.8
trans,*trans*-ON·OO·NO	**26**	33.8	36.6	31.4
cis,*cis*-OO·$(NO)_2$	**27**	48.3	47.2	
trans,*trans*-OO·$(NO)_2$	**28**	66.3	60.7	

[a] The bracketed values were determined to have a single imaginary frequency indicative of their being transition states (kcal/mol). [b] Reference 73.

by a weakly bound pair of NO_2 radicals. The dissociation energy of sym-N_2O_4 in the gas phase is 75 kJ/mol. The characteristic bands for symmetric NO_2 are 1368−1359 cm^{-1}, and for antisymmetric NO_2 they are 1758−1730 cm^{-1}. As well, a very strong out-of-plane NO_2 bend is observed at 743 cm^{-1}.[67]

$$N_2O_4 \leftrightarrow 2NO_2 \quad \text{(I)}$$

$$N_2O_4(l) \leftrightarrow NO^+(l) + NO_3^-(l) \quad \text{(II)}$$

$$N_2O_4(l) \leftrightarrow NO_2^+(l) + NO_2^-(l) \quad \text{(III)}$$

In anhydrous solutions, N_2O_4 self-ionizes almost completely to NO^+ and NO_3^- (reaction II) and, to a much lesser degree, to NO_2^+ and NO_2^- (reaction III). Partial dissociation of sym-N_2O_4 occurs in solution at low temperatures but becomes complete above 140 °C.[65] Sym-N_2O_4 is known to undergo self-ionization endothermically to form *trans*-ON·O·NO_2 **19** and *cis*-ON·O·NO_2 **18s**. Isomer **18s** is usually observed in condensed phases as a minor contaminant of sym-N_2O_4. Sterling et al.[74] describes the formation of **19** as the combination NO_2 and NO linked through an O bridge. The IR bands of **19** are 1290 cm^{-1} for the symmetric stretch of NO_2, 1644 cm^{-1} for the antisymmetric stretch of NO_2, and 1828 cm^{-1} for the N═O stretching mode.[67]

Perpendicular perp-ON·O·NO_2 **21** is found to have an O−N−O−NO dihedral angle of 90° for the terminal nitroso group (−N═O) relative to the planar NO_3 group, whereas for *cis*-ON·O·NO_2 **18s** and twist-ON·O·NO_2 **18g** we see dihedral angles of 6.8° and 40.1°, respectively.[76] Upon optimization, isomers **18s** and **18g** are found to interconvert into each other on going from the gas phase to solution and back again. Therefore, **18s** is not found to exist in the gas phase, and **18g** is not found to exist in the solution phase. Although these three conformations may appear to be very similar in structure, upon closer inspection of their bond lengths one sees that they are substantially different. The IR bands of **18g** are 1290 cm^{-1} for the symmetric stretch of NO_2, 1584 cm^{-1} for the antisymmetric stretch of NO_2, and 1890 cm^{-1} for the N═O stretching mode.[67] As for NO_2·O_2N **23**, Olson et al.[73] found it to be a stable intermediate to the formation of the more stable **21**.

The structural parameters for isomers ON·O_2NO **20** and $NO^+NO_3^-$ **22** are calculated for the first time, as far as we can determine. However, the X-ray crystal structure of $N_4O_6^{2+}$ potentially contains **20** and **22** as structural subcomponents.[76,77] We believe that Song et al.[78] discusses the formation of **22** as a high pressure and high temperature induced phase transition from sym-N_2O_4 to ionic $NO^+NO_3^-$. They identify an observed IR peak at 2208 cm^{-1} as the distinguishing feature correlating it with the experimentally observed NO^+ stretching mode at 2390−2102 cm^{-1}.[67,79] Our DFT/B3LYP/cc-pVTZ calculations yielded a stretching mode of 2167 cm^{-1}, underestimating the result of Song et al. by 41 cm^{-1}. This is a reasonable deviation, considering that DFT/B3LYP/cc-pVTZ is known to underestimate frequencies by around this amount.

The peroxide form ON·OO·NO has been proposed as an intermediate in the oxidation of NO by O_2 to yield NO_2.[73] Its three conformations are cis/cis, cis/trans, and trans/trans **24**−**26**. The remaining isomer type OO·$(NO)_2$ is believed to have been calculated for the first time and was found to come in two conformational forms cis/cis **27** and trans/trans **28**.

B. Classifications of UN_4O_{12} Isomers Containing Uranyl Nitrate. Using the p5 B3LYP gas-phase optimized relative Gibbs free energy results we were able to visually sort the optimized gas-phase geometries of 73 distinct UN_4O_{12} isomers into three separate categories: (1) 44 dinitrogen tetroxide adducts of uranyl nitrate, $UO_2(NO_3)_2$·N_2O_4, (2) 22 nitrosonium salt adducts of uranyl nitrate $NO^+UO_2(NO_3)_3^-$, $NO^+UO_2(NO_3)_2O(NO_2)^-$, $NO^+UO_2(NO_3)_2(ONOO)^-$, or $(NO^+)_2UO_2(NO_3)_2O_2^{2-}$, and (3) seven bis(nitrogen dioxide) adducts of uranyl nitrate, $UO_2(NO_3)_2$·$2NO_2$. Our first category, the a-series, is characterized by having various forms of a neutral N_2O_4 group attached to a neutral uranyl nitrate. Basically, any weakly bound combination of two nitrogens and four oxygens not considered to be part of the uranyl nitrate group fell into this category. Fourteen a-series types were identified. The second category, the b-series, is characterized by the existence of a NO^+ group thought to be ionically bound to a complex anion $[UN_3O_{11}]^-$. Four different b-series types were identified. The third category, the c-series, consists of two NO_2 groups that are not bound to each other but are each separately attached to uranyl nitrate. Only the one c-series type was identified.

N_2O_4 Adducts. A total of 44 gas-phase optimized structures were located for the a-series category of the UN_4O_{12} isomers, $UO_2(NO_3)_2$·N_2O_4 (Figures 3 and 4 and the Supporting Information). They contain the lowest gas-phase Gibbs free energy isomer **a1**, which we chose to use as the reference for the comparison of the Gibbs free energy differences of all of the gas-phase isomers calculated. Fourteen different types of N_2O_4 adducts of uranyl nitrate were identified; all but six (types 3, 4, 8, 9, 13, and 14) were found to contain N_2O_4 structural forms

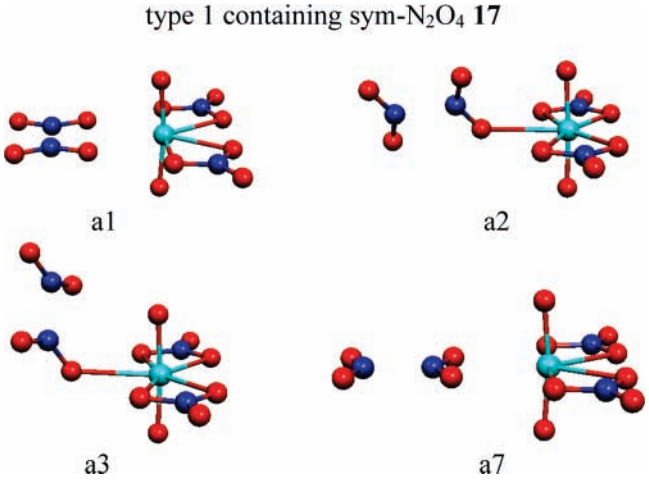

Figure 3. Optimized UN_4O_{12} isomers: uranyl nitrate N_2O_4 adducts (bound NO_2 groups) obtained from p5 PBE/cc-pVTZ gas-phase optimized geometries.

previously identified in papers by Olson et al.[73] (types 1, 2, 5, 6, and 10−12), McKee et al.[75] (types 1, 6, 7, and 12), and Wang et al.[80] (types 1, 6, 7, and 10−12).

The most stable and most commonly cited gas- and solution-phase form of sym-N_2O_4 **17** was not only found to be represented within the three most stable gas-phase UN_4O_{12} structures but was also determined to have four separate type 1 orientations (**a1**, **a2**, **a3**, and **a7**) (Figure 3). Both **a1** "side-on" and **a7** "end-on" are bidentately bound to uranium in the equatorial plane, whereas both **a2** and **a3** are unidentately bound.

The third most stable solution-phase form of free N_2O_4, *trans*-ON·O·NO_2 **19**, was determined to be a component of four distinct type 6 orientations of UN_4O_{12} (Figure 4). Only **a5** was found to bond bidentately to uranium. The lowest-energy variation was **a4** with a G_{gas}^{rel} value of 2.1 kcal/mol. All three of **a4**, **a10**, and **a11** were found to be unidentately bound to uranium.

cis-ON·O·NO_2 **18s** is considered to be the second most stable solution-phase form of free N_2O_4. Six versions of the type 7 UN_4O_{12} isomer with **18s** as a component were identified with **a6** found to be lowest in energy with a G_{gas}^{rel} value of 2.7 kcal/mol. The others are **a9**, **a12**, and **a15**−**a17**.

The fourth most stable solution-phase form ON·O_2NO **20** first occurs within type 8 as **a8** with a gas-phase relative Gibbs free energy of 2.6 kcal/mol and then also unidentately bound to uranium as **a13** and **a14** and again in an inverted form with the nitroso (−N═O) group oxygen unidentately bound to uranium as **a34** and **a35**.

Two occurrences of type 9, **a27** and **a44**, containing $NO^+NO_3^-$ **22**, the sixth most stable solution form of free N_2O_4, were identified, similar structurally to those of type 8, except the type 9 isomers contain an inverted nitrosonium cation instead of a nitroso (−N═O) group. Isomer **a27** corresponds to an inverted nitrosonium version of **a8**. The energy found for **a27** is 18.5 kcal/mol.

Nitrosonium Salts. A total of 22 gas-phase optimized structures were located for this b-series category of the UN_4O_{12} isomers, $NO^+UO_2(NO_3)_3^-$, $NO^+UO_2(NO_3)_2O(NO_2)^-$, $NO^+UO_2(NO_3)_2(ONOO)^-$, or $(NO^+)_2UO_2(NO_3)_2O_2^{2-}$. They contain the fourth and fifth lowest gas-phase Gibbs free energy isomers **b1** and **b2**. Four distinct types of nitrosonium salts were identified.

The first set of five type 15 isomers **b1**−**b4** and **b6**, Figure 5, was found to have the lowest relative Gibbs free energies within the b-series. The first four structures were quite close in gas-phase energy to that of the reference structure **a1** with **b1** having a G_{gas}^{rel} value of 1.4 kcal/mol.

$2NO_2$ Adducts. Seven c-series type 19 isomers **c1**−**c7** were identified with a uranyl nitrate group and two completely separate NO_2 groups located in various energy minimizing positions, $UO_2(NO_3)_2{\cdot}2NO_2$.

A more extensive version of the preceding discussion can be found in the Supporting Information under the same heading, in particular, the UN_4O_{12} isomers with high relatively energies: a-series types 3−5, 7−9, and 14, b-series types 16−18, and c-series type 19.

C. General Analysis and Discussion of Select UN_4O_{12} Isomers. Single-point solvated Gibbs free energies were calculated for 30 gas-phase optimized structures (**a1**−**a21**, **a27**, **b1**−**b7**, and **c1)** with g03 B3LYP/CPCM using the p5 PBE gas-phase optimized geometries (Table 1). We chose to focus on the 22 UN_4O_{12} isomers **a1**−**a16**, **a27**, **b1**−**b4**, and **b6** after determining that they represented the 22 most stable structures in solution as well as the 20 most stable structures in the gas phase. The two isomers not among the 20 most stable gas-phase isomers are **a27** and **b6**. With the two largest ΔG_{solv} values of −31.5 and −31.1 kcal/mol, they were found to go from being the 33rd and 27th most stable isomers in the gas phase to being the fifth and 14th most stable isomers in solution.

A general analysis and discussion of the nature of bonding, Gibbs relative free energies, dipole moments, bond lengths, angles, and orders, Hirschfeld atomic charges,[81,82] vibrational frequencies, and metal coordination are given to provide the reader with a general understanding of how these properties varied over the selected UN_4O_{12} isomers.

Nature of Bonding within the N_2O_4 Unit and between NO^+ and $UO_2(NO_3)_3^-$ Components. In performing an analysis of the various structures it was deemed important to discuss the nature of the bonding within the identified complexes. Often this can be subject to different interpretations, so the following outlines the approach we chose to use in our interpretation.

There are various potential ways leading to the formation of these structures. In the following, we will describe a likely scenario. In solution our three starting components are uranium, present as the uranyl dication, dinitrogen tetroxide mostly in the sym-N_2O_4 form, and nitromethane, which is responsible for the dissociation of sym-N_2O_4 into the ionic components NO^+ and NO_3^-, reaction II. With the anionic nitrate available, both uranyl nitrate $UO_2(NO_3)_2$ and trinitratouranylate $UO_2(NO_3)_3^-$ are expected to form. Next, the abundant sym-N_2O_4 likely combines with uranyl nitrate to form the a-series type 1 isomers **a1**−**a3** and **a7** in varying amounts. Furthermore, the combination of a nitrosonium cation and a trinitratouranylate complex anion likely leads to the formation of the b-series type 1 isomers **b1**−**b4** and **b6** as well as the a-series isomers **a5**, **a6**, **a8**, and **a27**. The remaining a-series isomers (**a4** and **a9**−**a16**), if at all existent in solution, could be formed through isomerization of the other forms.

Upon the basis of the abundance of research available on sym-N_2O_4, which consists of two radical NO_2 groups forming a biradical covalent N−N bond, the four a-series type 1 isomers **a1**−**a3** and **a7** containing sym-N_2O_4 are considered to be of covalent bonding character with respect to their N−N bond. As described above, these UN_4O_{12} complexes are thought to be the result of coordinate bonding between neutral N_2O_4 and uranyl nitrate components.

The five b-series type 1 isomers **b1**−**b4** and **b6** all contain a nitrate anion (NO_3^-) attached to a neutral uranyl nitrate forming

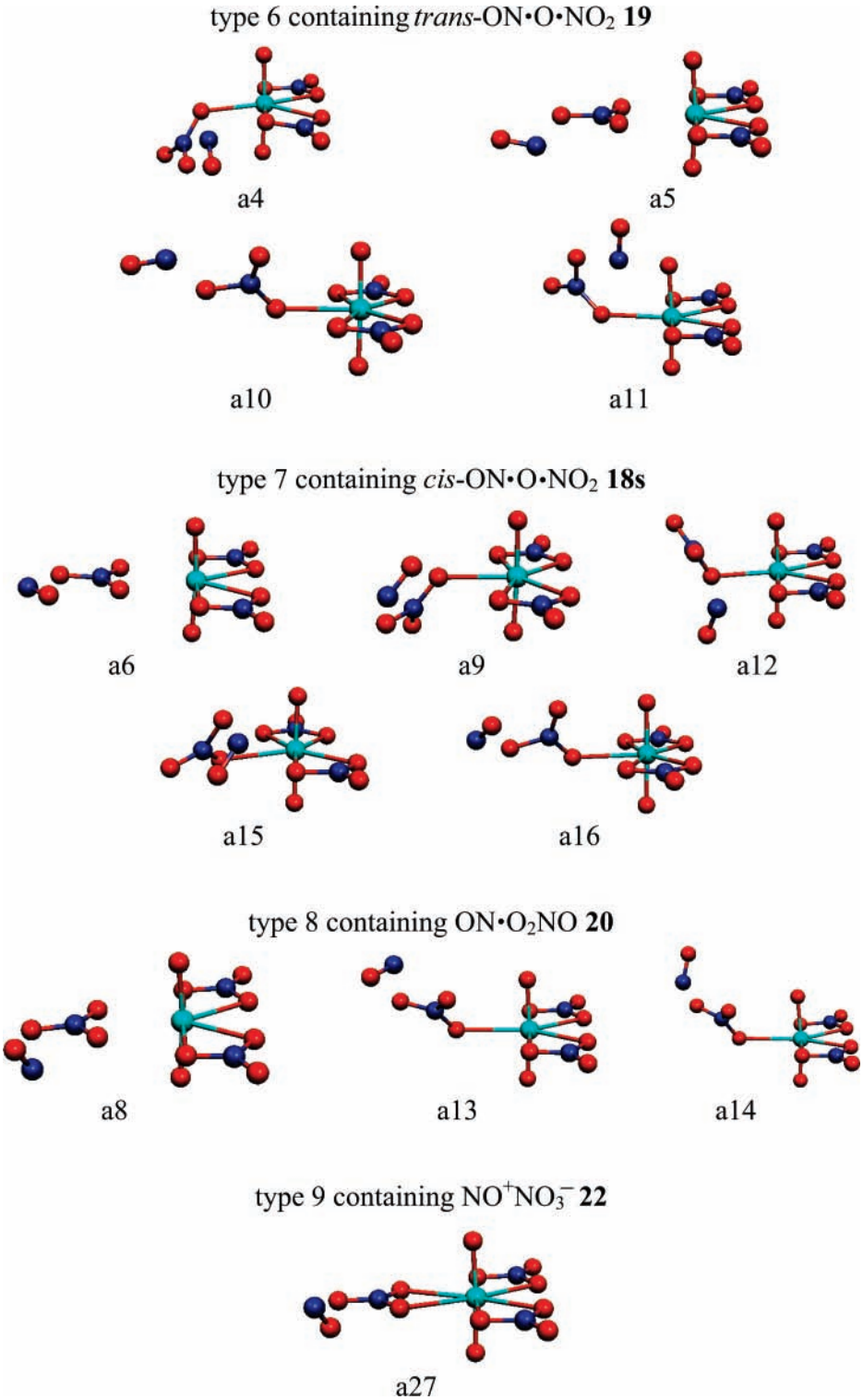

Figure 4. Optimized UN_4O_{12} isomers: uranyl nitrate N_2O_4 adducts (NO_3 bound to a terminal nitroso (−N═O) or inverted nitrosonium cation) obtained from p5 PBE/cc-pVTZ gas-phase optimized geometries.

the complex anion $[UO_2(NO_3)_3]^-$, which further combines with a nitrosonium cation (NO^+) in various ways (Figure 5). At first glance, all of these b-series type 1 isomers should be predominantly of ionic bonding character and are described as salts or salt adducts of uranyl nitrate. However, this is not necessarily the case as we discuss in more detail below.

For the remaining 18 isomers, we have defined the O_x oxygen to be the one that is weakly bound to the nitrogen of N_y═O except for **a27** and **b6** where two O_x oxygens bond symmetrically to the oxygen of N_y═O. N_y═O is considered to be a nitrosonium cation or an inverted nitrosonium cation (**b6**) for the b-series isomers and a terminal nitroso (−N═O) group or an inverted nitrosonium cation (**a27**) for the a-series isomers. The key bond for characterizing the nature of bonding of these structures is the O_x−N_y or O_x−O bond.

Isomer **b6** has a unique structure that involves an inverted N_y═O^+ group with its oxygen bonded symmetrically to two separate nitrate oxygens of uranyl nitrate. More importantly, isomer **b6** is considered to be the only one of the b-series type 1 isomers to be ionic in character. It has an O_x−O bond length

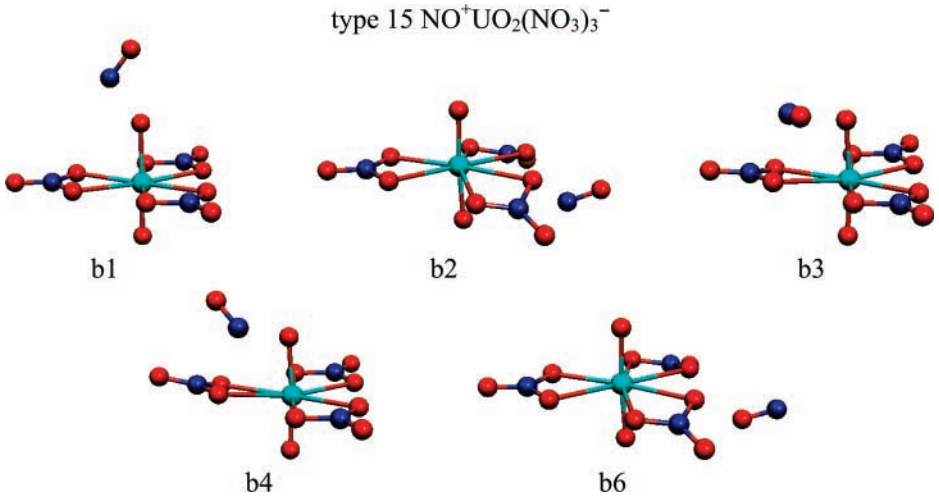

Figure 5. Optimized UN_4O_{12} isomers: uranyl nitrate nitrosonium salt adducts obtained from p5 PBE/cc-pVTZ gas-phase optimized geometries.

of 2.364 Å, an O_x−O bond order of 0.10, a N_y═O bond length of 1.105 Å, a N_y═O bond order of 2.41, and a N_y═O frequency of 2025 cm^{-1}. Corresponding experimental and theoretical values are 1.15 Å, 2.5 ,and 1876 cm^{-1} for free NO and 1.06 Å, 3.0, and 2390−2102 cm^{-1} for free NO^+.

Isomers **b2**, **b3**, and **b4**, classified as salts, are considered to be mostly ionic in nature. They have a small amount of covalent bonding character in the O_x−N_y bond with bond lengths of 2.127, 2.158, and 2.213 Å and bond orders of 0.29, 0.26, and 0.23, respectively. However, isomer **b1** with the shortest O_x−N_y bond length (1.735 Å) and a corresponding bond order of 0.65 may be more appropriately described as of mixed covalent/ionic character rather than an ionic salt, although it is still considerably more ionic than covalent.

Isomer **a27** of type 9 has a unique structure that involves an inverted N_y═O^+ group with its oxygen bonded symmetrically to two different oxygens of a nitrate group. It is considered to be the only one of the selected a-series isomers to be predominantly of ionic character. It has an O_x−O bond length and bond order of 2.375 Å and 0.09 as well as a N_y═O bond length, bond order, and frequency of 1.109 Å, 2.37, and 2007 cm^{-1}.

The calculated data also show that the a-series type 8 isomers **a8**, **a13**, and **a14**, containing a N_2O_4 component of the form ON·O_2NO have O_x−N_y bond lengths of 2.110, 2.097, and 2.085 Å and corresponding bond orders of 0.28, 0.33, and 0.33. These isomers, therefore, represent the a-series isomers of mixed covalent/ionic bonding character with the most ionic character.

The remaining nine a-series type 6 and 7 isomers **a4**−**a6**, **a9**−**a12**, **a15**, and **a16** containing a N_2O_4 component of the form *trans*- or *cis*-ON·O·NO_2 are interpreted to be of mixed covalent/ionic bonding character, ranging in O_x−N_y bond length from 1.783 to 2.039 Å and in O_x−N_y bond order from 0.67 to 0.39 for **a10** and **a12**, respectively (Figure 4).

Energies. The 20 most stable gas-phase isomers are all within 5.45 kcal/mol (**a16**) of the gas-phase reference. The same 20 isomers in solution become much more separated from each other and are now found to be within 10.4 kcal/mol (**a15**) of the solution-phase reference. Also noticeable is that the order of the gas-phase relative Gibbs free energies is not maintained in solution; a substantial reorganization of the 20 most stable gas-phase isomers has occurred. As well, the solvent can be seen to have a stabilizing effect on the external charge distribution for the isomers analyzed; all 22 analyzed structures show a substantial reduction in absolute Gibbs free energy in going from the gas to the solution phase, with $\Delta G_{solv} = -12.8$ kcal/mol (**a2**) or more and on average $\Delta G_{solv} = -18.3$ kcal/mol (Table 1).

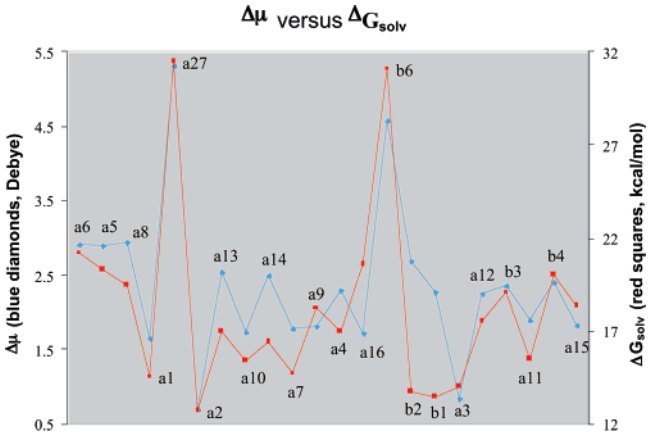

Figure 6. $\Delta\mu$ (diamonds, debye) versus ΔG_{solv} (squares, kcal/mol) of 22 UN_4O_{12} isomers.

Dipole Moments. The two plots presented in Figure 6 of the differences in the gas- and solution-phase dipole moments $\Delta\mu = \mu_{soln} - \mu_{gas}$ and the solvation free energies ΔG_{solv} provide a rough estimate of the ionic versus covalent nature of the bonding within the 22 UN_4O_{12} isomers. The two most ionic isomers, with the largest values of $\Delta\mu$ and ΔG_{solv}, are **a27** and **b6**, whereas **a1** and **a2**, with the smallest changes in dipole moment and solvation free energies, would be considered the least ionic or the most covalent. Figure 6 provides some indication of the ionic versus covalent nature of these isomers, and a general correlation can been seen between $\Delta\mu$ and ΔG_{solv}. Both the amount of reduction in ΔG_{solv} and the order in relative Gibbs free energies of the 22 selected isomers can be attributed in part to the degree of charge separation within these particular structures. This charge separation is represented to a first order by the permanent dipole moment. In the gas phase both the p5 and g03 B3LYP results for dipole moments are very similar with the largest variance of 0.28 D (**a27**) found over the 22 isomers. The two isomers with the lowest and highest dipole moments in both the gas and the solution phases are **a2** and **a27**, respectively. The change in dipole moment $\Delta\mu$ is always positive in going from the gas phase to the solution phase. The change is reasonably consistent, ranging from 0.70 (**a2**) to 5.31 D (**a27**) but averaging 2.36 D for the 22 isomers. Higher-order charge moments will certainly play a role as well.

TABLE 3: Calculated Bond Lengths and Angles Using p5 PBE/cc-pVTZ Gas-Phase Optimized Geometries of the 22 Most Stable Solution-Phase UN_4O_{12} Isomers (in angstroms and deg)

	uranyl nitrate						dinitrogen tetroxide / nitrosonium salt						
isomers	U═O	U═O	U−O	O_U−N	N−O_t	OUO	U−O	O_U−N	O_x−N_y[a]	N_y═O	N−N	UON	O_UNO
a6	1.797	1.796	2.423	1.306	1.203	174.2	2.653	1.252	1.938	1.115		96.2	119.5
a5	1.796	1.797	2.425	1.305	1.203	174.0	2.665	1.243	1.862	1.120		95.2	119.9
a8	1.796	1.796	2.421	1.306	1.202	174.4	2.657	1.303	2.110	1.115		97.6	117.6
a1	1.795	1.796	2.419	1.309	1.201	172.6	2.762	1.211			1.864		
a27	1.795	1.795	2.458	1.295	1.207	176.5	2.540	1.298	2.375	1.109			
a2	1.793	1.791	2.444	1.301	1.201	177.4	2.599	1.226			1.881		
a13	1.793	1.796	2.404	1.311	1.202	175.2	2.556	1.250	2.097	1.119			
a10	1.794	1.792	2.451	1.300	1.202	178.2	2.538	1.249	1.783	1.128			
a14	1.798	1.792	2.405	1.311	1.202	174.9	2.541	1.251	2.085	1.119			
a7	1.795	1.795	2.414	1.308	1.201	172.5	2.820	1.214			1.884		
a9	1.794	1.795	1.445	1.300	1.201	176.4	2.449	1.278	1.934	1.114			
a4	1.792	1.795	2.397	1.312	1.200	176.4	2.382	1.294	1.993	1.118			
a16	1.793	1.792	2.448	1.300	1.202	178.9	2.539	1.250	1.838	1.123			
b6	1.794	1.799	2.541	1.277	1.207	176.6			2.364	1.105		96.6	123.3
b2	1.792	1.798	2.567	1.266	1.201	176.2			2.127	1.115		96.6	123.5
b1	1.968	1.795	2.415	1.305	1.199	179.9			1.735	1.126		96.9	123.5
a3	1.799	1.790	2.445	1.301	1.200	176.2	2.568	1.231			1.897		
a12	1.793	1.793	2.396	1.318	1.200	175.9	2.387	1.305	2.039	1.117			
b3	1.877	1.793	2.412	1.307	1.200	174.6			2.158	1.113		96.4	120.5
a11	1.831	1.790	2.391	1.314	1.200	176.2		1.287	1.956	1.117			
b4	1.893	1.792	2.411	1.308	1.199	174.9			2.213	1.116		96.4	120.8
a15	1.790	1.790	2.433	1.302	1.200	178.5	2.515	1.268	1.906	1.120			
exptl.[b]		1.753	2.456	1.291	1.203	179.8						96.5	123.0

[a] O_x oxygen bonds weakly to nitrogen of N_y═O except for **a27** and **b6** where it bonds to oxygen of N_y═O. [b] Reference 26 for $NO^+UO_2(NO_3)_3^-$ in the solid state.

TABLE 4: Calculated Gas-Phase Bond Orders Using p5 PBE/cc-pVTZ Optimized Geometries of the 22 Most Stable Solution-Phase UN_4O_{12} Isomers

	uranyl nitrate					dinitrogen tetroxide/nitrosonium salt				
isomers	U═O	U═O	U−O	O_U−N	N−O_t	U−O	O_U−N	O_x−N_y[a]	N_y═O	N−N
a6	2.39	2.39	0.57	1.28	1.72	0.26	1.47	0.50	2.34	
a5	2.39	2.39	0.56	1.28	1.72	0.26	1.51	0.56	2.31	
a8	2.39	2.39	0.57	1.28	1.72	0.23	1.28	0.28	2.32	
a1	2.40	2.40	0.58	1.27	1.72	0.18	1.63			0.38
a27	2.39	2.39	0.51	1.31	1.70	0.35	1.30	0.09	2.37	
a2	2.40	2.40	0.54	1.30	1.73	0.24	1.58			0.37
a13	2.39	2.40	0.59	1.26	1.73	0.31	1.46	0.33	2.29	
a10	2.40	2.40	0.54	1.30	1.73	0.32	1.46	0.67	2.27	
a14	2.39	2.40	0.59	1.26	1.73	0.32	1.45	0.33	2.29	
a7	2.40	2.40	0.58	1.27	1.73	0.17	1.65			0.36
a9	2.39	2.40	0.54	1.30	1.73	0.40	1.35	0.50	2.35	
a4	2.40	2.40	0.59	1.26	1.73	0.53	1.29	0.43	2.30	
a16	2.40	2.40	0.54	1.30	1.73	0.32	1.45	0.61	2.28	
b6	2.39	2.39	0.39	1.37	1.70	0.55	1.28	0.10	2.41	
b2	2.39	2.40	0.36	1.42	1.73	0.57	1.28	0.29	2.33	
b1	1.95	2.41	0.58	1.27	1.74	0.44	1.12	0.65	2.34	
a3	2.39	2.40	0.54	1.30	1.73	0.27	1.53			0.35
a12	2.40	2.39	0.59	1.26	1.73	0.54	1.26	0.39	2.32	
b3	1.95	2.41	0.58	1.27	1.74	0.44	1.12	0.26	2.34	
a11	2.19	2.40	0.61	1.25	1.74	0.49	1.32	0.46	2.32	
b4	1.88	2.41	0.58	1.27	1.74	0.44	1.15	0.23	2.32	
a15	2.40	2.40	0.55	1.29	1.73	0.38	1.39	0.50	2.29	

[a] O_x oxygen bonds weakly to nitrogen of N_y═O except for **a27** and **b6** where it bonds to oxygen of N_y═O.

Bond Lengths, Angles, Bond Orders, and Atomic Charges. For structural analysis each of the 22 selected isomers was separated into uranyl nitrate and nitrosonium tetroxide or nitosonium salt fragments. Ten bonds and three angles were identified for analysis (Tables 3 and 4).The gas-phase uranyl bond lengths were found to vary little when no external group was found binding to either of the axial uranyl oxygens. In this case, they span a range of 1.790−1.799 Å, averaging around 1.795 Å. Correspondingly, the uranyl bond orders were very consistent at 2.40 ± 0.01. These numbers correspond to the well-known partial triple bond character of the uranyl bond. The uranyl bond order is reduced to values below 2.0 for those cases where a NO^+ is attached to the uranyl oxygen (**b1**, **b3**, and **b4**). All of the select gas-phase N_y═O bond lengths are found to range from 1.105 to 1.128 Å, with an average of 1.117 Å.

As for the weak O_x−N_y bond, it plays an important role in identifying the degree of charge separation between the N_y═O cation and the O_x oxygen of the complex anion for the isomers with ionic components. Equatorial U−O(nitrate) bonds show bond orders of 0.5−0.6 in most cases, corresponding to partial covalent character, whereas the U−O(N_2O_4) bond orders are in most cases lower, averaging 0.36.

TABLE 5: Calculated Hirschfeld Atomic Charges Using p5 PBE/cc-pVTZ Gas-Phase Optimized Geometries of the 22 Most Stable Solution-Phase UN_4O_{12} Isomers (in e)

	uranyl nitrate						dinitrogen tetroxide/nitrosonium salt				
isomers	U	$O_{U=O}$	$O_{U=O}$	O_U	N	O[a]	O_U	N[b]	O_x[c]	N_y	$O_{N=O}$
a6	0.49	−0.29	−0.28	−0.16	0.30	−0.14	−0.12	0.30	−0.05	0.24	0.16
a5	0.49	−0.28	−0.28	−0.16	0.30	−0.14	−0.10	0.30	−0.12	0.24	0.14
a8	0.49	−0.28	−0.29	−0.16	0.30	−0.14	−0.10	0.30	−0.12	0.24	0.15
a1	0.51	−0.28	−0.28	−0.17	0.30	−0.13	−0.03	0.25			
a27	0.48	−0.28	−0.28	−0.15	0.30	−0.13	−0.14	0.29	−0.16	0.25	0.21
a2	0.60	−0.28	−0.27	−0.16	0.30	−0.13	−0.05	0.23			
a13	0.56	−0.29	−0.28	−0.16	0.30	−0.14	−0.10	0.30	−0.13	0.22	0.13
a10	0.58	−0.29	−0.28	−0.16	0.30	−0.14	−0.09	0.30	−0.12	0.21	0.11
a14	0.56	−0.30	−0.27	−0.16	0.30	−0.14	−0.10	0.30	−0.12	0.22	0.13
a7	0.51	−0.28	−0.28	−0.16	0.30	−0.16	−0.15	0.22			
a9	0.56	−0.28	−0.28	−0.16	0.30	−0.13	−0.15	0.30	−0.13	0.24	0.17
a4	0.57	−0.27	−0.29	−0.16	0.30	−0.13	−0.16	0.30	−0.14	0.24	0.13
a16	0.58	−0.28	−0.28	−0.16	0.30	−0.14	−0.09	0.30	−0.12	0.22	0.12
b6	0.48	−0.28	−0.30	−0.11	0.29	−0.15	−0.15	0.30	−0.17	0.27	−0.15
b2	0.48	−0.27	−0.30	−0.11	0.30	−0.13	−0.15	0.30	−0.15	0.25	0.15
b1	0.47	−0.28	−0.26	−0.15	0.30	−0.12	−0.15	0.30	−0.25	0.26	0.17
a3	0.57	−0.30	−0.27	−0.16	0.30	−0.13	−0.06	0.23			
a12	0.56	−0.28	−0.28	−0.16	0.30	−0.13	−0.17	0.30	−0.14	0.24	0.14
b3	0.47	−0.28	−0.26	−0.15	0.30	−0.12	−0.15	0.30	−0.28	0.26	0.17
a11	0.55	−0.30	−0.26	−0.16	0.30	−0.12	−0.15	0.30	−0.14	0.25	0.14
b4	0.48	−0.28	−0.25	−0.15	0.30	−0.12	−0.15	0.29	−0.28	0.27	0.15
a15	0.58	−0.28	−0.27	−0.15	0.30	−0.13	−0.11	0.29	−0.11	0.23	0.13

[a] External O of uranyl nitrate. [b] N of N_2O_4 or NO_3 nearest to U. [c] O_x oxygen bonds weakly to nitrogen of N_y═O except for **a27** and **b6** where two O_x oxygens bond to oxygen of N_y═O.

Of all of the isomers studied, structure **b1** was found to be the closest in geometry to that of the crystal structure isolated.[26] Unsigned mean deviations of selected bond lengths and angles between experimental X-ray crystallography and gas-phase calculations of 0.035 Å/0.3° were obtained. In particular, the experimental uranyl bond length is 1.753 Å, which is 0.042 Å less than the calculated average. This shows that the PBE XC functional with the cc-pVTZ basis set used in our study overestimates this type of bond length, in agreement with earlier findings.[42,83] In studying UF_6 in the gas phase, Batista et al.[44] determined that using a PBE functional with a 6-31+G* basis set overestimated bond lengths by 1−2%. In our gas-phase study using PBE and cc-pVTZ, we found that the uranyl bond lengths were overestimated on average by 2.4%. This is reasonable considering the larger sizes of the structures analyzed.

The calculated U and O charges in the uranyl ion vary little among the different species (Table 5). With the exception of **b6**, all selected UN_4O_{12} b-series isomers contain a N_y═O group where both atoms are positively charged. The nitrosonium oxygen of **b6** is the only one that was negatively charged.

Frequencies. Analysis of gas-phase frequencies for the 22 selected isomers highlights the predominantly mixed covalent/ionic nature of the majority of these isomers (Table 6). Particularly distinct dinitrogen tetroxide/nitrosonium salt bands are the N_y═O stretching modes, the two N_y═O torsions, the O_x−N_y stretching mode, and the out-of-plane NO_3 bending mode.

Experimentally, the gas-phase stretching frequency of N═O in its free form is 1876 cm^{-1},[84] and as part of **18g**, 1890 cm^{-1}, and **19**, 1828 cm^{-1}. However, N═O^+ in its free form exhibits frequencies ranging from 2390 to 2102 cm^{-1} and in salts is often seen to absorb in the 2391−2150 cm^{-1} range.[85] The 18 isomers that we studied with N_y═O stretching frequencies had values that ranged from 1915 to 2025 cm^{-1}, suggesting that the complexation of these structures had the effect of shortening/strengthening the N_y═O bond relative to their N_2O_4 counterparts in free form, thereby increasing the N_y═O stretching frequencies. The actual effect may even be somewhat larger because DFT PBE has a tendency to underestimate experimental values.

In general, other than the strongly mixed modes of **a2**, we see a very consistent underestimation of uranyl symmetric and antisymmetric stretching modes (848 ± 7 and 930 ± 7 cm^{-1}) and an overestimation of the uranyl bending mode (203 ± 6 cm^{-1}) across all isomers analyzed. This can be compared to experimental IR spectral data[86] where we see gas-phase values of 871, 940, and 182 cm^{-1}, resulting in differences of −24, −12, and +23 cm^{-1}, respectively. Exceptions are the uranyl bending mode of **a12**, **a27**, and **b6** and the uranyl modes of **a11**. As for the b-series, with the bonding of NO^+ to one of the uranyl oxygens in **b1, b3**, and **b4** the typical uranyl modes do not exist; in their place we see lone U═O stretching and bending modes. This is not, however, the case with **b2** and **b6** where the nitrosonium ion bonds symmetrically between two nitrate oxygens.

Coordination Numbers. Of all of the isomers studied, coordination to uranium was always found to be either seven- or eight-coordinate. Seven-coordinate uranium was found to contain a unidentately coordinated component, and eight-coordinate uranium was found to contain a bidentately coordinated component. The one exception is **c7**, which was found to contain two unidentately coordinated components for a coordination of 8.

D. By-Type Discussion of Selected UN_4O_{12} Isomers. This final subsection focuses on a by-type discussion of 22 select UN_4O_{12} isomers for the purpose of identifying the structure or structures most likely to predominate in either an inert gas or a nonaqueous polar aprotic solvent environment. To gauge the likelihood of their existence in the gas or solution phases, UN_4O_{12} isomers were tabulated according to their relative Gibbs free energies. Of the 22 selected structures, only two of the three categories and six of the 19 types classified in subsection B were represented. The proceeding discussions are organized around these six types of isomers: a-series type 1, 6, 7, 8, and 9 and b-series type 1.

TABLE 6: Calculated Vibrational Frequencies Using p5 PBE/cc-pVTZ Gas-Phase Optimized Geometries of the 22 Most Stable Solution-Phase UN_4O_{12} Isomers (cm^{-1})

	uranyl			dinitrogen tetroxide/nitrosonium salt											
isomers	s-str OUO	a-str OUO	bend OUO	s-str NO_2	a-bend NO_2	s-bend NO_2	s-str N−N	str NO_3	str NO_3	s-str NO_3	bend NO_3	str O_x−N_y[a]	str N_y=O	tor N_y=O	tor N_y=O
a6	843	923	203					1198	1423		758	289	1957	512	
a5	844	924	206					1201	1444		766	280	1933	522	
a8	846	926	208					1186	1419	974	760	267	1981	490	378
a1	846	925	200	1371	620	389	292								
a27	846	927	214										2007	278	252
a2[b]															
a13	849	929	208					1208	1355	999	769	274	1961	517	399
a10	851	933	207					1202	1579		745	319	1920	501	
a14	847	928	209					1213	1347	999	771	277	1962	514	393
a7	850	927	197	1383	729	418	273								
a9	849	931	208					1120	1530		764	308	1991	515	
a4	850	932	209					1107	1504		772	279	1963	477	330
a16	852	934	206					1196	1508		764	324	1941	572	
b6	842	925	225										2025	277	261
b2	846	929	206									263	1980	468	376
b1												269	1915	652	583
a3	848	930		1369	724	375	264								
a12	849	932	221					1090	1506		772		1965	463	
b3												297	1984	458	370
a11	789	905	224					1122	1512		761	275	1968	482	296
b4												317	1964	459	346
a15	855	937	207					1162	1481		783	333	1943	548	256
exptl.[c]	871	940	182												

[a] O_x oxygen bonds weakly to nitrogen of N_y=O except for **a27** and **b6** where it bonds to oxygen of N_y=O. [b] Strongly mixed vibrational modes for **a2**. [c] Reference 86 for $NO^+UO_2(NO_3)_3^-$ in the solid state.

*a-Series Type 1: **a1**, **a2**, **a3**, and **a7**.* All four a-series type 1 isomers are found to be among the 20 most stable gas-phase and the 22 most stable solution-phase isomers. This group is characterized by containing the most stable gas-phase form of planar sym-N_2O_4 (Figure 3). Bidentately bound planar N_2O_4 components within **a1** and **a7** maintain their planar form with the equatorial plane of uranyl nitrate, whereas unidentately bound planar N_2O_4 components within **a2** and **a3**, although equatorially bound to uranium, maintain their planar shape outside the equatorial plane of uranyl nitrate.

With **a2** being within 0.2 kcal/mol of **a1** for our p5 B3LYP gas-phase calculations and actually lower than **a1** by 0.2 kcal/mol for the g03 B3LYP gas-phase calculations, it is quite possible that **a2** is the more stable isomer. In any case, at room temperature both are as likely to be present. The remaining two isomers **a3** and **a7** have p5 gas-phase relative Gibbs free energies of 1.2 and 2.5 kcal/mol, respectively. In solution these four isomers become the fourth, sixth, 17th, and 10th most stable with relative Gibbs free energies of 3.6, 5.2, 9.0, and 6.8 kcal/mol, respectively. The absolute Gibbs free energy differences between the gas- and the solution-phase results for these four isomers are found to be less than average (−18.3 kcal/mol), ranging from −12.8 to −14.7 kcal/mol with **a2** having the lowest ΔG_{solv} value of −12.8 kcal/mol. The dipole moment differences between the gas and the solution phases are also found to be below average (2.36 D), ranging from 0.70 to 1.78 D.

The two longest U−O bonds, 2.762 Å for **a1** and 2.820 Å for **a7**, both connect uranium bidentately to N_2O_4. Correspondingly, we see the two smallest bond orders of 0.18 for **a1** and 0.17 for **a7**. The O_U−N bond lengths for **a1** and **a7** are 1.211 and 1.214 Å due to bidentately bound N_2O_4 components, whereas for **a2** and **a3** they are 1.226 and 1.231 Å due to unidentately bound N_2O_4 components. These four bonds correspond to the four strongest O_U−N bond orders overall, 1.63, 1.58, 1.53, and 1.65 for **a1**, **a2**, **a3**, and **a7**, respectively. The four weakly binding N−N bonds were found to have values of 1.864, 1.881, 1.897, and 1.884 Å and bond orders of 0.38, 0.37, 0.35, and 0.36 for **a1**, **a2**, **a3**, and **a7**. As for the atomic charges, only those on uranium showed a significant variation with 0.51 for both bidentate isomers (**a1** and **a7**) and 0.60 and 0.57 for the two unidentate isomers **a2** and **a3**.

Four characteristic vibrational modes, one NO_2 stretching mode and two NO_2 bending modes along with one N−N stretching mode, were used to analyze three of the four a-series type 1 isomers. The lower-frequency out-of-plane antisymmetric bending mode of **a1** could be used to distinguish it from **a3** and **a7**. Otherwise the two NO_2 bonded radicals of **a1**, **a3**, and **a7** were found to have similar stretching and bending modes. Isomer **a2** has many mixed modes, and it was found to be very difficult to identify any distinct modes.

*a-Series Type 6: **a4**, **a5**, **a10**, and **a11**.* All four a-series type 6 isomers are found to be among the 22 selected isomers. This group is characterized by containing various orientations of *trans*-ON·O·NO_2 **19**. Only **a5** was found to bond bidentately to uranium. In comparing bond lengths of the N_2O_4 component of **a5** to those of free N_2O_4, we see that 1.862, 1.243, and 1.120 Å compare to 1.61, 1.20, and 1.13 Å for O_xN_y, O_U−N, and N_y=O. Of these, only the O_x−N_y bond distance, with a difference of 0.25 Å, does not compare well. This is perhaps due to the inability of the DFT/GGA/cc-pVTZ method to model this bond correctly. In going from the gas phase to solution isomers **a4**, **a5**, **a10**, and **a11** change from having relative Gibbs free energies of 2.1, 2.4, 3.0, and 3.7 kcal/mol to values of 7.4, 1.1, 6.0, and 10.0 kcal/mol. With **a5** being only 1.1 kcal/mol above **a6**, it is considered to be a reasonably good candidate to exist and predominate in solution. The ΔG_{solv} values show little variation from the average of −18.3 kcal/mol, ranging from −15.4 to −20.3 kcal/mol. The change in dipole moment, $\Delta\mu$, ranges from 1.73 to 2.90 for these isomers but does not vary significantly from the average value of 2.36 D.

As for the structural analysis of this series of isomers as well as the atomic charges and vibrational frequencies, they were found to be very similar, and no distinguishing features could be identified.

a-Series Type 7: ***a6***, ***a9***, ***a12***, ***a15***, *and* ***a16***. Five of the possible six isomers of the a-series type 7 are found to be among the 22 selected isomers with the other isomer **a17** being the 23rd most stable isomer in solution. This group is characterized by containing *cis*-ON·O·NO_2 **18s**.

Isomer **a6**, with a gas-phase relative Gibbs free energy of 2.5 kcal/mol, was determined to be the most stable isomer in solution overall and as such is thought to be the most likely isomer to exist and predominate in solution. In comparing bond lengths of the N_2O_4 component of **a6** to those of free N_2O_4, we see that 1.938, 1.252, and 1.115 Å compare very well to 1.93, 1.23, and 1.09 Å for O_xN_y, O_U-N, and $N_y=O$. Other features of **a6** are that it is the only type 7 isomer bidentately bound to uranium and that it along with **a9** contains the only two nearly planar forms of *cis*-ON·O·NO_2. As for the other type 7 isomers (**a12**, **a15**, and **a16**) their N_2O_4 components are found to be noticeably less planar. In going from the gas to the solution phase, the remaining isomers (**a9**, **a12**, **a15**, and **a16**) have relative Gibbs free energies of 2.9, 4.1, 4.8, and 5.5 kcal/mol and 6.8, 9.1, 10.4, and 7.6 kcal/mol, respectively. The values for ΔG_{solv}, μ, and $\Delta\mu$ are quite similar for these isomers and change little from their average values with the exception of the dipole moment of **a6**, which at 12.63 D is the second largest.

The U−O bond length of **a6** is just over 0.1 Å longer than the other four isomers due to its bidentate bonding to uranium. Correspondingly, the bond order is about 0.06 less for **a6**. The atomic charges of the dinitrogen tetroxide component are found to be very similar for all five isomers.

As for the vibrational frequencies, all are very much the same, and no characterizing information could be identified. In particular, distinguishing **a6** from **a5** would be very difficult as nearly every mode tabulated for these two isomers is in close agreement. The $N_y=O$ stretching mode provides the largest frequency difference of +24 cm^{-1} for **a6** relative to that of **a5**.

a-Series Type 8: ***a8***, ***a13***, *and* ***a14***. Three of the five members of the a-series type 8 isomers are found to be among the 22 selected isomers. This group is characterized by containing ON·O_2NO **20** where the nitrogen of a nitrosonium cation bonds symmetrically to two oxygens of a nitrate group.

The only bidentate isomer is **a8** with gas- and solution-phase relative Gibbs free energies of 2.6 and 2.2 kcal/mol, respectively. Isomer **a8** is the third most stable solution-phase isomer and possibly a candidate to exist in solution. In comparing bond lengths of the N_2O_4 component of **a8** to those of free N_2O_4, we see that 2.110, 1.303, and 1.115 Å compare reasonably well to 2.03, 1.28, and 1.11 Å for O_x-N_y, O_U-N, and $N_y=O$. The other two type 8 isomers are also found to be quite stable in solution with **a13** and **a14** being the sixth and eighth most stable at 5.6 and 6.3 kcal/mol compared to their gas-phase energies of 4.5 kcal/mol each. The ΔG_{solv}, μ, and $\Delta\mu$ values are quite similar and change little from their average values.

The U−O bond length of **a8** is just over 0.1 Å longer than the other two type 8 isomers due to its bidentate bonding to uranium. Correspondingly, the bond order is about 0.08 less for **a8**. As for the atomic charges of the dinitrogen tetroxide component, they are very similar for all three isomers.

The most identifying vibrational frequency of these three isomers is the symmetric stretching mode of the non-uranyl nitrate NO_3 group (974 cm^{-1} for **a8** and 999 cm^{-1} for both **a13** and **a14**), which is not seen for the other selected isomers.

a-Series Type 9: ***a27***. Only one of two possible isomers of a-series type 9 **a27** was found to be among the selected isomers. This type is characterized by containing an ionically bound $NO^+NO_3^-$ **22** component, where uncharacteristically the oxygen of a nitrosonium cation bonds symmetrically to two oxygens of a nitrate group. Isomer **a27** with gas- and solution-phase relative Gibbs free energies of 17.8 and 4.5 kcal/mol, respectively, is the fifth most stable solution-phase UN_4O_{12} isomer. The **a27** isomer is found to have the largest values for ΔG_{solv} = −31.5 kcal/mol, μ_{gas} = 14.44 D, μ_{soln} = 20.03 D, $\Delta\mu$ = 5.31 D, and O_x-N_y bond length = 2.375 Å of all 22 selected isomers.

Isomer **a27** has many similarities with **b6**; for example, both have a nitrosonium ion that is inverted with the oxygen of the NO^+ group, bonding equally to the two nitrate oxygens. As well, they represent the two isomers with the largest values for ΔG_{solv}, $\Delta\mu$, and O_x-N_y bond lengths. Furthermore, they share three very similar characteristic vibrational modes: the $N_y=O$ stretching band and the two $N_y=O$ torsion bands. Both are also found to have the two highest $N_y=O$ stretching frequencies corresponding to the two shortest $N_y=O$ bond lengths. The one area where they differ substantially is the atomic charge on the $O_{N=O}$ oxygen, Table 5, where **a27** is seen to have the largest positive charge of 0.21 e and **b6** is seen to have the lowest charge of −0.15 e (the only one found to be negatively charged).

b-Series Type 15: ***b1***, ***b2***, ***b3***, ***b4***, *and* ***b6***. All five b-series type 15 nitrosonium salt adducts of uranyl nitrate are found to be among the 20 most stable gas-phase and the 22 most stable solution-phase isomers. This group is characterized by containing a NO^+ group ionically bound to a $[UO_2(NO_3)_3]^-$ complex anion. For isomer **b1**, the nitrogen of the NO^+ cation is bound to one of the uranyl oxygens. Similarly, for **b3** and **b4**, the nitrogen of the nitrosonium ion appears to be weakly shared between both the nitrate oxygen and the uranyl oxygen. As for isomers **b2** and **b6**, they share a similar symmetric configuration with the NO^+ group ionically shared between two different nitrate oxygens. With **b2**, the nitrogen of the nitrosonium ion is bound to the two nitrate oxygens, whereas in the case of **b6** the nitrosonium ion is inverted with the oxygen of the NO^+ group bonding equally to the two nitrate oxygens.

The fourth and fifth lowest gas-phase relative Gibbs free energy isomers are **b1** and **b2** with relative Gibbs free energies of 1.4 and 1.7 kcal/mol. They become the 15th and 14th isomers in solution with relative Gibbs free energies of 8.2 and 8.8 kcal/mol, respectively. The other isomers **b3, b4**, and **b6** have G_{gas}^{rel} values of 2.6, 3.6, and 15.7 kcal/mol in the gas phase and 9.6, 10.4, and 8.2 kcal/mol in solution. The ΔG_{solv} values of these five b-series isomers show the largest variation ranging from −13.5 kcal/mol for **b1** to −31.1 kcal/mol for **b6**. As for the change in dipole moment values, $\Delta\mu$, they are all found to be near the 2.36 D average for the selected isomers with the highest b-series type 15 $\Delta\mu$ of 4.58 D for **b6**.

The interaction of the NO^+ group with the uranyl oxygens leads to a weakening and therefore a lengthening of the uranyl bond lengths for **b1** (1.877 Å), **b3** (1.968 Å), and **b4** (1.893 Å) compared to the average of 1.795 Å. This is supported by smaller corresponding uranyl bond orders of 1.95, 1.95, and 1.88 relative to the average of 2.40 (as discussed previously). All five b-series type 15 isomers were found to have the lowest atomic charges on uranium (0.47 or 0.48 e).

With the b-series type 15 isomers containing an anionic trinitratouranylate, we are able to identify four characteristic vibrational modes: one N=O stretching band, two N=O torsion bands, and one O_xN_y stretching band. Isomers **b1** and **b6** were

found to have the lowest and highest N═O stretching frequencies of 1915 and 2025 cm^{-1}, corresponding to the longest and shortest N_y═O bond lengths of 1.126 and 1.105 Å.

E. Dissociation. While not the main focus of the paper, we will briefly discuss the dissociation of UN_4O_{12} according to the following reaction

$$UN_4O_{12} \leftrightarrow [UO_2(NO_3)_3]^- + NO^+ \qquad \text{(IV)}$$

We have calculated the free energies for reaction IV using the exact same computational protocol as before. Taking for the left-hand side of reaction IV the most stable gas-phase isomer **a1**, we find free energies for the reaction of 120.7, 102.8, and 100.9 kcal/mol for p5 PBE, p5 B3LYP, and g03 B3LYP, respectively. Not surprisingly, the dissociation reaction is highly unfavorable in the gas phase.

In solution, we have taken the most stable solution-phase isomer **a6** as the reference point. At the previously used g03 CPCM B3LYP level of theory, we obtain a reaction energy of $\Delta G = -5.2$ kcal/mol. At that level of theory, the dissociated species, at infinite separation, would be more stable than the most stable undissociated conformer, and dissociation would be energetically favorable. The dramatic change between the gas and solution phases can be understood by the stabilization of the charged species in a polar solvent.

However, continuum solvation models such as those used here are at or beyond the limits of their applicability for molecules with a high concentration of charge, such as the NO^+ in our case. In other words, the solvation treatment is not entirely balanced between the small and the large molecules in reaction IV, introducing fairly large errors. Moreover, the situation in real, experimental solutions is likely to be even more complex than that modeled here. For instance, the possibility of ion pairs has not been accounted for by our simple solvation model. Overall, these errors make any conclusion regarding the relative stability of dissociated versus undissociated species questionable. One could create a somewhat more balanced model by including an explicit first solvation sphere or by applying dynamic methods. However, this is clearly outside the scope of the current investigation.

IV. Conclusions

The combination of the experimental and computational results obtained by others and the computational results generated for this paper have provided us with a much broader view of the structures involved and we believe a better insight into the likely identity of the predominant UN_4O_{12} uranyl nitrate isomer existing in both the gas phase and the 30:70 nitromethane/dinitrogen tetroxide solution used in experiment.[26]

In this paper, we have studied the relative Gibbs free energies of 73 identified UN_4O_{12} uranyl nitrate isomers. Fourteen of these isomers are closely spaced within 2.6 kcal/mol of the most stable gas-phase isomer **a1**. Isomer **a1** contains the most familiar and well-studied sym-N_2O_4 bidentately bound to the uranium atom of uranyl nitrate. The next most stable isomer **a2** was determined to be 0.2 kcal/mol more energetic by one method (p5 B3LYP) and 0.2 kcal/mol less energetic by our other method (g03 B3LYP). Isomer **a2** contains a unidentately bound form of sym-N_2O_4. The following three isomers in order of stability are **a3**, **b1**, and **b2** with relative Gibbs free energies of 1.2, 1.4, and 1.7 kcal/mol, according to the p5 B3LYP calculations. Isomer **a3** is a higher-energy conformation of **a2**, and the conformers **b1** and **b2** are the two most stable nitrosonium salt adducts of uranyl nitrate. For **b1** the nitrosonium ion is bound via nitrogen to one of the uranyl oxygens, and for **b2** the nitrosonium nitrogen is symmetrically bound between two oxygens of two different nitrate groups. On the basis of our relative Gibbs free energy results, all five of these isomers (**a1**, **a2**, **a3**, **b1**, and **b2**) are considered to be strong candidates to exist and possibly predominate in the gas phase, with **a1** and **a2** being the strongest candidates.

After narrowing down our relative Gibbs free energy calculations of 30 isomers in solution to the 22 most stable, we identified three isomers to be within 3.6 kcal/mol of the most stable solution-phase isomer **a6**. Isomer **a6** contains a *cis*-ON·O·NO_2 **18s** bidentately bound to uranyl nitrate. The next most stable isomer in solution **a5** (with a relative Gibbs free energy of 1.1 kcal/mol) contains the *trans*-ON·O·NO_2 **19** bidentately bound to uranyl nitrate. The third most stable isomer in solution is **a8** with a relative Gibbs free energy of 2.2 kcal/mol. Isomer **a8** is characterized by containing ON·O_2NO **20,** where the nitrogen of a terminal nitroso group bonds symmetrically to two oxygens of a nitrate group that is bidentately bound to uranium. The fourth most stable isomer in solution is **a1** with a relative Gibbs free energy of 3.6 kcal/mol. Therefore, isomer **a6** is considered to be the most likely candidate to predominate in a solution of nitromethane/dinitrogen tetroxide.

Of the 22 analyzed isomers, only two UN_4O_{12} isomers **a27** and **b6** were considered to clearly contain an O_x-N_y ionic bond with the two largest bond lengths of 2.375 and 2.364 Å, respectively. Also, these two isomers represented the two largest N_y═O stretching frequencies of 2007 cm^{-1} for **a27** and 2025 cm^{-1} for **b6**, corresponding to the two shortest bond lengths of 1.109 to 1.105 Å. Four isomers, **a1**−**a3** and **a7**, containing sym-N_2O_4 isomers, had biradical covalent character, and therefore no N_y═O stretching frequencies were present. The remaining 12 dinitrogen tetroxide adducts and four nitrosonium salt adducts of uranyl nitrate had mixed covalent/ionic character with N_y═O stretching frequencies that ranged from 1915 to 1991 cm^{-1} and corresponding bond lengths ranging from 1.113 to 1.128 Å.

Although the **b1** structure was found to most closely describe the geometry of the solid-state crystals prepared,[26] the 8.8 kcal/mol relative Gibbs free energy in solution suggests that **b1** is not a likely candidate to predominate in solution. All five of the nitrosonium salt adducts of uranyl nitrate that were within the 22 most stable solution-phase isomers were at least 8.2 kcal/mol (**b6**) more energetic than the reference **a6** and therefore are not thought to be likely candidates to predominate in solution.

Experimentally with the lowering of the temperature of the saturated solution and upon solidification[26] it seems quite possible for the terminal nitroso or nitrosonium cation group of any one of the 18 isomers mentioned (Figures 4 and 5) with ionic or mixed covalent/ionic character to have rearranged into the solid-state crystal structure that was identified as the nitrosonium salt, $NO^+UO_2(NO_3)_3^-$.

The question of dissociation in solution has been addressed briefly by applying a simple model reaction. However, the results are inconclusive.

It is important to recognize that the computational methods used do not take into account such factors as reaction kinetics, pH levels in solution, or solute/solvent concentrations, and the necessary approximations of the methods are sources of error that create some uncertainty in the interpretation of the results obtained. What the computational methods do provide are structural relative Gibbs free energies that approach chemical

accuracy, which can be used as a measure of relative stability for identifying those structures found to be the most computationally stable. Thus, in providing experimentalists with strong candidates, along with accompanying molecular properties, it is our hope that it will prove to be useful in identifying the existence of these UN_4O_{12} structures within both the solution and the gas phases.

For this study, the use of optimized gas-phase geometries to calculate single-point relative Gibbs free energies in solution is not ideal and may be a possible source of error. Optimizing these geometries in solution would be preferable, though current methods present difficulties with convergence.

Also, there is an inherent difficulty in modeling weak bonds, such as the O_x-N_y or O_x-O bond, found in 18 of the selected isomers, as well as the N−N bonds found in the remaining four isomers. This along with the known tendency for DFT PBE to overestimate bond lengths is a likely source of some error. Correspondingly, the longer bond lengths translate into an underestimation of vibrational frequencies. As well, there may be some error in the use of DFT B3LYP for calculating absolute Gibbs free energies; however, due to the benefit of error cancellation a smaller degree of error would be seen for relative Gibbs free energies. It is reassuring, however, that the lowest solution-phase isomers are all a-series N_2O_4 adducts. Moreover, the same general conclusion would emerge from using DFT with the PBE functional, again giving some confidence in our results.

The use of restricted, closed-shell formalism may not model some of the higher-energy structures effectively due to the biradical nature of some of the N_2O_4 isomers and the UN_4O_{12} isomers containing them as components.

Furthermore, the inclusion of spin−orbit relativistic effects may be enough to change the ordering of relative Gibbs free energy results in the gas phase because many of the low-energy isomers are so closely spaced in energy. This is less likely in solution due to the larger gaps in relative Gibbs free energies. However, with all of the U^{VI} structures analyzed being of the f^0 type, spin−orbit effects may not be a significant factor.

Acknowledgment. J.J.B. thanks M. A. Namdarghanbari for many helpful discussions. G.S. acknowledges Drs. J. D. Xidos and P. H. M. Budzelaar, University of Manitoba, for valuable comments. We are grateful to Dr. D. N. Laikov, Moscow/Stockholm, for making his Priroda code available to us. Financial support from the Natural Sciences and Engineering Research Council of Canada and from the University of Manitoba start-up funds and The Research Grants Program are gratefully acknowledged.

Supporting Information Available: Additional discussions of sections A and B for the UN_4O_{12} isomers beyond the 22 focused on above as well as structures in Figures 7−12, Table 7 containing the complete compilation of the relative Gibbs free energies of all 73 UN_4O_{12} isomers, and Table 8 showing the data on dipole moments and $\Delta\mu = \mu_{soln} - \mu_{gas}$ for the 22 UN_4O_{12} isomers. This material is available free of charge via the Internet at http://pubs.acs.org.

References and Notes

(1) Pepper, M.; Bursten, B. E. *Chem. Rev.* **1991**, *91*, 719.

(2) Dolg, M. Lanthanides and actinides. In *Encyclopedia of Computational Chemistry*; Schleyer, P. v. R., Allinger, N. L., Clark, T., Gasteiger, J., Kollman, P. A., Schaefer, H. F., III, Schreiner, P. R., Eds.; Wiley Interscience: Chichester, 1998; pp 1478−1486.

(3) Schreckenbach, G.; Hay, P. J.; Martin, R. L. *J. Comput. Chem.* **1999**, *20*, 70.

(4) Kaltsoyannis, N. *Chem. Soc. Rev.* **2003**, *32*, 9.

(5) Vallet, V.; Macak, P.; Wahlgren, U.; Grenthe, I. *Theor. Chem. Acc.* **2006**, *115*, 145.

(6) Clark, D. L.; Hobart, D. E.; Neu, M. P. *Chem. Rev.* **1995**, *95*, 25.

(7) *The Chemistry of the Actinide and Transactinide Elements*, 3rd ed.; Morss, L. R., Edelstein, N. M., Fuger, J., Eds.; Springer: Dordrecht, The Netherlands, 2006.

(8) Streitwieser, A. *Inorg. Chim. Acta* **1984**, *94*, 171.

(9) Sonnenberg, J. L.; Hay, P. J.; Martin, R. L.; Bursten, B. E. *Inorg. Chem.* **2005**, *44*, 2255.

(10) Kaltsoyannis, N.; Scott, P. *The f Elements*; Oxford University Press: New York, 1999.

(11) Taylor, J. C.; Mueller, M. H. *Acta Crystallogr.* **1965**, *19*, 536.

(12) Dalley, N. K.; Mueller, M. H.; Simonsen, S. H. *Inorg. Chem.* **1971**, *10*, 323.

(13) Hughes, K. A.; Burns, P. C. *Acta Crystallogr., Sect. C: Cryst. Struct. Commun.* **2003**, *59*, I7.

(14) Ruas, A.; Bernard, O.; Caniffi, B.; Simonin, J. P.; Turq, P.; Blum, L.; Moisy, P. *J. Phys. Chem. B* **2006**, *110*, 3435.

(15) Pasilis, S.; Somogyi, A.; Herrmann, K.; Pemberton, J. E. *J. Am. Soc. Mass. Spectrom.* **2006**, *17*, 230.

(16) Kaplan, L.; Hildebrandt, R. A.; Ader, M. *J. Inorg. Nucl. Chem.* **1956**, *2*, 153.

(17) Krivovichev, S. V.; Burns, P. C. *Radiochemistry* **2004**, *46*, 16.

(18) Blackwell, L. J.; King, T. J.; Morris, A. *J. Chem. Soc., Chem. Commun.* **1973**, *17*, 644.

(19) Dehnicke, K.; Strahle, J. *Chem. Ber.* **1964**, *97*, 1502.

(20) Addison, C. C. *Chem. Rev.* **1980**, *80*, 21.

(21) Tikhomirov, G. A.; Znamenkov, K. O.; Morozov, I. V.; Kemnitz, E.; Troyanov, S. I. *Z. Anorg. Allg. Chem.* **2002**, *628*, 269.

(22) Brouard, M.; Cireasa, R.; Clark, A. P.; Preston, T. J.; Vallance, C. *J. Chem. Phys.* **2006**, *124*.

(23) Tolbert, M. a.; Rossi, M. J.; Golden, D. M. *Science* **1988**, *240*, 1018.

(24) Wayne, R. P.; Barnes, I.; Biggs, P.; Burrows, J. P.; Canosamas, C. E.; Hjorth, J.; Lebras, G.; Moortgat, G. K.; Perner, D.; Poulet, G.; Restelli, G.; Sidebottom, H. *Atmos. Environ., Part A* **1991**, *25*, 1.

(25) Brown, S. S.; Osthoff, H. D.; Stark, H.; Dube, W. P.; Ryerson, T. B.; Warneke, C.; de Gouw, J. A.; Wollny, A. G.; Parrish, D. D.; Fehsenfeld, F. C.; Ravishankara, A. R. *J. Photochem. Photobiol., A* **2005**, *176*, 270.

(26) Crawford, M. J.; Mayer, P. *Inorg. Chem.* **2005**, *44*, 8481.

(27) Addison, C. C.; Champ, H. A. J.; Hodge, N.; Norbury, A. H. *J. Chem. Soc.* **1964**, 2354.

(28) Koch, W.; Holthausen, M. C. *A Chemist's Guide to Density Functional Theory*; Wiley-VCH: New York, 2000.

(29) Cramer, C. J. *Essentials of Computational Chemistry: Theories and Models*, 2nd ed.; Wiley: Hoboken, NJ, 2004.

(30) Tsipis, C. A. *Comments Inorg. Chem.* **2004**, *25*, 19.

(31) Hay, P. J.; Martin, R. L.; Schreckenbach, G. *J. Phys. Chem. A* **2000**, *104*, 6259.

(32) Laikov, D. N. *Chem. Phys. Lett.* **1997**, *281*, 151.

(33) Laikov, D. N. An implementation of the scalar relativistic density functional theory for molecular calculations with Gaussian basis sets. Poster presentation, *DFT2000 Conference*, Menton, France; 2000.

(34) Laikov, D. N. *Chem. Phys. Lett.* **2005**, *416*, 116.

(35) Laikov, D. N.; Ustynyuk, Y. A. *Russ. Chem. Bull.* **2005**, *54*, 820.

(36) Frisch, M. J.; Trucks, G. W.; Schlegel, H. B.; Scuseria, G. E.; Robb, M. A.; Cheeseman, J. R.; Montgomery, J. A., Jr.; Vreven, T.; Kudin, K. N.; Burant, J. C.; Millam, J. M.; Iyengar, S. S.; Tomasi, J.; Barone, V.; Mennucci, B.; Cossi, M.; Scalmani, G.; Rega, N.; Petersson, G. A.; Nakatsuji, H.; Hada, M.; Ehara, M.; Toyota, K.; Fukuda, R.; Hasegawa, J.; Ishida, M.; Nakajima, T.; Honda, Y.; Kitao, O.; Nakai, H.; Klene, M.; Li, X.; Knox, J. E.; Hratchian, H. P.; Cross, J. B.; Bakken, V.; Adamo, C.; Jaramillo, J.; Gomperts, R.; Stratmann, R. E.; Yazyev, O.; Austin, A. J.; Cammi, R.; Pomelli, C.; Ochterski, J. W.; Ayala, P. Y.; Morokuma, K.; Voth, G. A.; Salvador, P.; Dannenberg, J. J.; Zakrzewski, V. G.; Dapprich, S.; Daniels, A. D.; Strain, M. C.; Farkas, O.; Malick, D. K.; Rabuck, A. D.; Raghavachari, K.; Foresman, J. B.; Ortiz, J. V.; Cui, Q.; Baboul, A. G.; Clifford, S.; Cioslowski, J.; Stefanov, B. B.; Liu, G.; Liashenko, A.; Piskorz, P.; Komaromi, I.; Martin, R. L.; Fox, D. J.; Keith, T.; Al-Laham, M. A.; Peng, C. Y.; Nanayakkara, A.; Challacombe, M.; Gill, P. M. W.; Johnson, B.; Chen, W.; Wong, M. W.; Gonzalez, C.; Pople, J. A. *Gaussian 03*; Gaussian, Inc.: Wallingford, CT, 2004.

(37) Perdew, J. P.; Burke, K.; Ernzerhof, M. *Phys. Rev. Lett.* **1996**, *77*, 3865.

(38) Becke, A. D. *J. Chem. Phys.* **1993**, *98*, 5648.

(39) Lee, C.; Yang, W.; Parr, R. G. *Phys. Rev. B: Condens. Matter* **1988**, *37*, 785.

(40) Stephens, P. J.; Devlin, F. J.; Chabalowski, C. F.; Frisch, M. J. *J. Phys. Chem.* **1994**, *98*, 11623.

(41) Küchle, W.; Dolg, M.; Stoll, H.; Preuss, H. *J. Chem. Phys.* **1994**, *100*, 7535.

(42) Shamov, G. A.; Schreckenbach, G. *J. Phys. Chem. A* **2005**, *109*, 10961.
(43) Shamov, G. A.; Schreckenbach, G.; Vo, T. *Chem.—Eur. J.* **2007**, *13*, 4932.
(44) Batista, E. R.; Martin, R. L.; Hay, P. J.; Peralta, J. E.; Scuseria, G. E. *J. Chem. Phys.* **2004**, *121*, 2144.
(45) Han, Y.-K.; Hirao, K. *J. Chem. Phys.* **2000**, *113*, 7345.
(46) Han, Y. K. *J. Comput. Chem.* **2001**, *22*, 2010.
(47) Schreckenbach, G.; Wolff, S. K.; Ziegler, T. *J. Phys. Chem. A* **2000**, *104*, 8244.
(48) Schreckenbach, G. *Int. J. Quantum Chem.* **2005**, *101*, 372.
(49) Straka, M.; Kaupp, M. *Chem. Phys.* **2005**, *311*, 45.
(50) Dyall, K. G. *J. Chem. Phys.* **1994**, *100*, 2118.
(51) Laikov, D. N. Ph.D. Thesis, Moscow State University, 2000.
(52) Cossi, M.; Rega, N.; Giovanni, S.; Barone, V. *J. Comput. Chem.* **2003**, *24*, 669.
(53) Fonseca, Guerra, C.; Snijders, J. G.; te Velde, G.; Baerends, E. J. *Theor. Chem. Acc.* **1998**, *99*, 391.
(54) te Velde, G.; Bickelhaupt, F. M.; Baerends, E. J.; Fonseca, Guerra, C.; van Gisbergen, S. J. A.; Snijders, J. G.; Ziegler, T. *J. Comput. Chem.* **2001**, *22*, 931.
(55) Baerends, E. J.; Autschbach, J.; Bérces, A.; Bo, C.; Boerrigter, P. M.; Cavallo, L.; Chong, D. P.; Deng, L.; Dickson, R. M.; Ellis, D. E.; Fan, L.; Fischer, T. H.; Fonseca Guerra, C.; van Gisbergen, S. J. A.; Groeneveld, J. A.; Gritsenko, O. V.; Grüning, M.; Harris, F. E.; van den Hoek, P.; Jacobsen, H.; van Kessel, G.; Koostra, F.; van Lenthe, E.; McCormack, D. A.; Osinga, V. P.; Patchkovskii, S.; Philipsen, P. H. T.; Post, D.; Pye, C. C.; Ravenek, W.; Ros, P.; Schipper, P. R. T.; Schreckenbach, G.; Snijders, J. G.; Sola, M.; Swart, M.; Swerhone, D.; te Velde, G.; Vernooijs, P.; Versluis, L.; Visser, O.; van Wezenbeek, E.; Wiesenekker, G.; Wolff, S. K.; Woo, T. K.; Ziegler, T. *ADF*, version 2004.01; Scientific Computing and Modelling, Theoretical Chemistry, Vrije Universiteit: Amsterdam, 2004.
(56) van Lenthe, E.; Baerends, E. J.; Snijders, J. G. *J. Chem. Phys.* **1993**, *99*, 4597.
(57) van Lenthe, E.; Baerends, E. J.; Snijders, J. G. *J. Chem. Phys.* **1994**, *101*, 9783.
(58) van Lenthe, E.; Ehlers, A.; Baerends, E. J. *J. Chem. Phys.* **1999**, *110*, 8943.
(59) van Lenthe, E.; van Leeuwen, R.; Baerends, E. J. *Int. J. Quantum. Chem.* **1996**, *57*, 281.
(60) Klamt, A.; Schüürmann, G. *J. Chem. Soc., Perkin Trans. 2* **1993**, 799.
(61) Klamt, A.; Jonas, V.; Bürger, T.; Lohrenz, J. C. W. *J. Phys. Chem. A* **1998**, *102*, 5074.
(62) Pye, C. C.; Ziegler, T. *Theor. Chem. Acc.* **1999**, *101*, 396.
(63) Charrin, N.; Moisy, P.; Blanc, P. *Radiochim. Acta* **2001**, *89*, 579.
(64) Bagnall, K. W.; Robinson, P. S.; Stewart, M. A. A. *J. Chem. Soc. A* **1961**, 4060.
(65) Cotton, F. A.; Wilkinson, G.; Murillo, C. A.; Bochmann, M. *Advanced Inorganic Chemistry*, 6th ed.; Wiley: New York, 1999.
(66) King, R. B. *Inorganic Chemistry of Main Group Elements*; Wiley-VCH: New York, 1995.
(67) Laane, J.; Ohlsen, J. R. Characterization of nitrogen oxides by vibrational spectroscopy. In *Progress in Inorganic Chemistry*; Wiley: New York, 1980; Vol. 27, pp 465−513.
(68) de Jong, W. A.; Harrison, R. J.; Nichols, J. A.; Dixon, D. A. *Theor. Chem. Acc.* **2001**, *107*, 22.
(69) de Jong, W. A.; Aprà, E.; Windus, T. L.; Nichols, J. A.; Harrison, R. J.; Gutowski, K. E.; Dixon, D. A. *J. Phys. Chem. A* **2005**, *109*, 11568.
(70) Slater, J. C. *Phys. Rev.* **1951**, *81*, 385.
(71) Vosko, S. H.; Wilk, L.; Nusair, M. *Can. J. Phys.* **1980**, *58*, 1200.
(72) Lebrero, M. C. G.; Perissinotti, L. L.; Estrin, D. A. *J. Phys. Chem. A* **2005**, *109*, 9598.
(73) Olson, L. P.; Kuwata, K. T.; Bartberger, M. D.; Houk, K. N. *J. Am. Chem. Soc.* **2002**, *124*, 9469.
(74) Stirling, A.; Papai, I.; Mink, J.; Salahub, D. R. *J. Chem. Phys.* **1994**, *100*, 2910.
(75) Mckee, M. L. *J. Am. Chem. Soc.* **1995**, *117*, 1629.
(76) Addison, C. C.; Blackwell, L. J.; Harrison, B.; Jones, D. H.; Logan, N.; Nunn, E. K.; Wallwork, S. C. *J. Chem. Soc., Chem. Commun.* **1973**, 347.
(77) Blackwell, L. J.; Nunn, E. K.; Wallwork, S. C. *J. Chem. Soc., Dalton Trans.* **1975**, 2068.
(78) Song, Y.; Hemley, R. J.; Mao, H. K. A.; Liu, Z. X.; Herschbach, D. R. *Chem. Phys. Lett.* **2003**, *382*, 686.
(79) Givan, A.; Loewenschuss, A. *J. Chem. Phys.* **1989**, *90*, 6135.
(80) Wang, X. F.; Qin, Q. Z. *Int. J. Quantum Chem.* **2000**, *76*, 77.
(81) Hirshfeld, F. L. *Theor. Chim. Acta* **1977**, *44*, 129.
(82) Guerra, C. F.; Handgraaf, J. W.; Baerends, E. J.; Bickelhaupt, F. M. *J. Comput. Chem.* **2004**, *25*, 189.
(83) Shamov, G. A.; Schreckenbach, G. *J. Phys. Chem. A* **2006**, *110*, 9486.
(84) Nakamoto, K. *Infrared Spectra of Inorganic and Coordination Compounds*, 2nd ed.; Wiley-Interscience: New York, 1970.
(85) Hadjiivanov, K. I. *Catal. Rev.* **2000**, *42*, 71.
(86) Kobets, L. V.; Klavsut, G. N.; Umreiko, D. S. *Zh. Neorg. Khim.* **1981**, *26*, 173.